Journal of
Medicinal Chemistry

Article

Discovery of Selective Small Molecule Degraders of BRAF-V600E

Xiao-Ran Han, Liqun Chen, Yuanqi Wei, Weihua Yu, Yanke Chen,
Chunyan Zhang, Bingyang Jiao, Tingting Shi, Lei Sun, Chao Zhang,
Yang Xu, Matthew R Lee, Ying Luo, Michael B. Plewe, and Jialiang Wang

J. Med. Chem., **Just Accepted Manuscript** • DOI: 10.1021/acs.jmedchem.9b02083 • Publication Date (Web): 30 Mar 2020

Just Accepted

is published by the American Chemical Society. 1155 Sixteenth Street N.W., Washington, DC 20036

Discovery of Selective Small Molecule Degraders of BRAF-V600E

Xiao-Ran Han,[†,§] Liqun Chen,[§] Yuanqi Wei,[§] Weihua Yu,[§] Yanke Chen,[§] Chunyan Zhang,[§] Bingyang Jiao,[§] Tingting Shi,[§] Lei Sun,[§] Chao Zhang,[§] Yang Xu,[§] Matthew R. Lee, [†] Ying Luo,[†] Michael B. Plewe,[†,*] Jialiang Wang [†,§,*]

[†]Cullgen Inc., 12671 High Bluff Drive Suite 130, San Diego, California 92130, USA. [§]Cullgen (Shanghai) Inc., Building 6, 230 ChuanHong Road, Chuansha, Pudong New Area, Shanghai 201202, People's Republic of China.

Abstract

BRAF is among the most frequently mutated oncogenes in human cancers. Multiple small molecule BRAF kinase inhibitors have been approved for treating melanoma carrying BRAF-V600 mutations. However, the benefits of BRAF kinase inhibitors are generally short lived. Small molecule-mediated targeted protein degradation has recently emerged as a novel pharmaceutical strategy to remove disease proteins through hijacking the cellular ubiquitin proteasome system (UPS). In this study, we developed thalidomide-based heterobifunctional compounds that induced selective degradation of BRAF-V600E, but not the wild type BRAF. Downregulation of BRAF-V600E suppressed the MEK/ERK kinase cascade in melanoma cells and impaired cell growth in culture. Abolishing the interaction between degraders and cereblon or blocking the UPS significantly impaired the activities of these degraders, validating a mechanistic role of UPS in mediating targeted degradation of BRAF-V600E. These findings highlight a new approach to modulate the functions of oncogenic BRAF mutants and provide a framework to treat BRAF-dependent human cancers.

Introduction

The rapidly accelerated fibrosarcoma (RAF) family of serine/threonine kinases, including ARAF, BRAF, and CRAF, transduce signals downstream of RAS to the mitogen-activated protein kinase (MAPK) cascade. They are the core components of a signal transduction network that supports proliferation and survival in mammalian cells.[1] Aberrations of BRAF are widely documented in human cancer, accounting for 6-8% of all cases.[2] In particular, almost half of melanoma and virtually all hairy cell leukemia are driven by BRAF mutations. While many forms of BRAF mutations have been identified, approximately 90% of these mutations convert the valine residue at codon 600 into a glutamic acid residue (i.e. V600E), which renders BRAF acting as a constitutively active monomer.[3] BRAF-V600E and other oncogenic BRAF mutants result in aberrant activation of the downstream MEK/ERK kinase cascade and other signaling pathways, thereby promoting oncogenesis.

To date, three BRAF kinase inhibitors, vemurafenib,[4] dabrafenib,[5] and encorafenib,[6] have been approved for treating melanoma patients carrying BRAF-V600 mutations. These inhibitors belong to the second generation of BRAF inhibitors that selectively target BRAF-V600 mutants and block activity of these proteins in monomeric forms. These BRAF kinase inhibitors have wide therapeutic windows because they spare dimeric wild type BRAF in normal tissues.[7] In addition, they are not active against other classes of BRAF mutants, such as BRAF fusions and splice variants.[8] Furthermore, the second-generation BRAF inhibitors are known to enhance formation of BRAF homodimer or heterodimers between BRAF and other RAF proteins.[1] This unique mechanism is thought to compromise clinical efficacy of these drugs, promote acquired resistance, and induce adverse effects, particularly induction of secondary skin cancer.[9] Nevertheless, vemurafenib and other approved BRAF

kinase inhibitors have produced marked response in melanoma patients with BRAF-V600 mutations.[10] The clinical benefits of currently approved BRAF kinase inhibitors are greatly restrained by rapid emergence of acquired resistance.[8] Combination with MEK inhibitors neutralizes the paradoxical activation of wild type BRAF induced by BRAF inhibitors, modestly improves response rate, and extends tumor control.[11] However, resistance and tumor recurrence remain inevitable. Approaches leading to more potent, selective and durable suppression of oncogenic BRAF mutants are expected to produce better tumor response and provide additional clinical benefits to patients.

Hijacking the ubiquitin proteasome system via heterobifunctional small molecule compounds is an emerging pharmaceutical strategy aiming to selectively remove disease-causing proteins in affected cells.[12] These small molecule degraders are also known as proteolysis-targeting chimeras (PROTACs), as these compounds comprise two recruiting ligands connected by a linker. One of the ligands binds to an E3 ubiquitin complex, and the other recruits the protein of interest (POI) to the E3 ligase complex. Once brought to close proximity of E3 ligases, the POI is polyubiquitinated and subsequently degraded by the proteasome. Targeted degradation of POIs not only compromises the catalytic activities of these proteins but also removes their scaffolding and other non-catalytic functions, providing unique advantages over inhibitors.

A growing list of disease-relevant proteins, mostly implicated in oncology, has been targeted by PROTAC molecules, such as BRD4, BRD9, ALK, and CDK4/6.[13-20] In the current study, we report two BRAF-V600E degraders generated from the E3 ligase ligand thalidomide and two BRAF kinase inhibitors, vemurafenib and BI882370.[21] These degraders selectively induced downregulation of BRAF-V600E in melanoma cells at nanomolar concentrations but not wild type BRAF, leading to

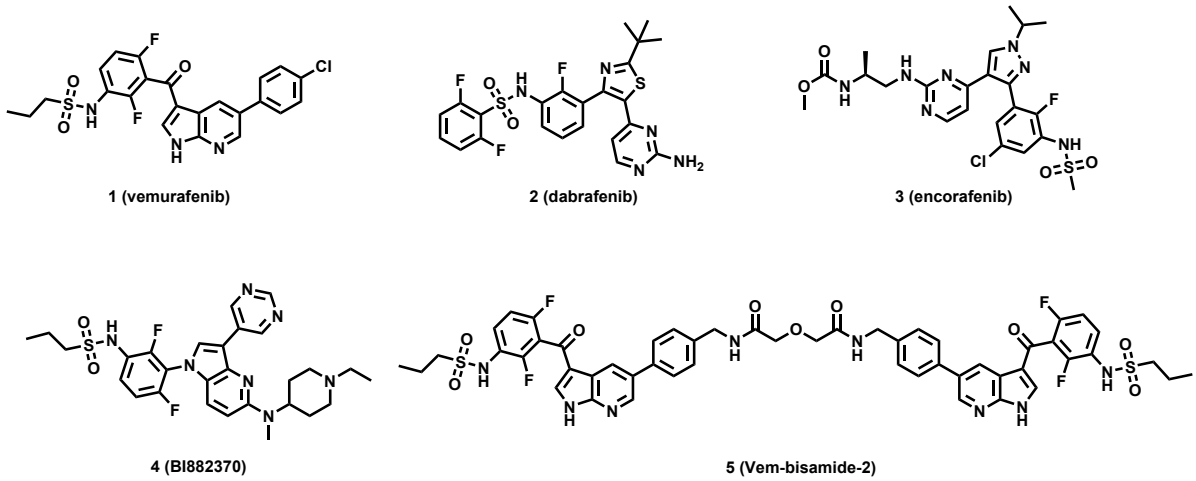

Figure 1. Chemical structures of **1** (vemurafenib), **2** (dabrafenib), **3** (encorafenib), **4** (BI882370) and **5** (Vem-bisamide-2).

growth arrest and apoptosis in target cells. Degradation of BRAF-V600E was verified to be dependent on the ubiquitin proteasome system. Thereby we demonstrated a novel therapeutic approach modulating oncogenic BRAF mutants at protein levels.

Results

Design and synthesis of BRAF degraders. From multiple reported BRAF kinase inhibitors[21] we selected vemurafenib and BI882370 as the BRAF binding moiety (Figure 1). Vemurafenib is the first approved BRAF kinase inhibitor for the treatment of late stage melanoma with threefold selectivity for BRAF-V600E over wild type BRAF,[22] while BI882370 is a more potent pan-RAF kinase inhibitor.[23] Co-crystal structures of BRAF in complex with vemurafenib (PDB ID: 3OG7) and with **5** (Vem-bisamide-2) (PDB ID: 5JT2)[24] show that part of the phenyl ring is solvent exposed allowing attachment of the linker. We connected the linker through an amide bond, with molecular modeling suggesting that the amide carbonyl group is capable of forming a hydrogen bond with the imidazole ring of His539 in BRAF-V600E (Supporting Figure S1). In the co-crystal structure of BRAF with BI882370 (PDB ID: 5CSX), the ethylpiperidinyl group is exposed to solvent and was exploited for

attachment of the linker. Besides the correct site of attachment, the choice of linker and E3-ligase ligand is critical for the development of effective PROTACs. In this study, a set of degraders varying in linkers and E3-ligase ligands was screened against BRAF-V600E (Supporting Figure S2-5), leading to the identification of two degraders of BRAF-V600E, namely **12** and **23**. In **12**, vemurafenib is attached to the E3 ligase ligand thalidomide at the meta-position through a pentanoyl linker. In **23**, using BI882370 as warhead, an 11-atom PEG linker was found to be the better choice (Scheme 1). We prepared **13** and **24** as the corresponding negative control compounds by *N*-methylation of the thalidomide moiety which disabled binding to cereblon.[15] We developed a convergent synthetic route for the synthesis of the designed BRAF degraders and their negative control compounds (Scheme 1). Suzuki coupling of **6** and **7**, followed by Boc deprotection afforded the vemurafenib analog **8** as the BRAF binding warhead. The thalidomide derivatives **11a** and **11b** were synthesized by nucleophilic aromatic substitution of the meta-fluoro-substituted thalidomide derivatives **9a** and **9b** with amino ester **10**, followed by *tert*-butyl ester deprotection. Amide coupling of **8** with **11a** and **11b** afforded **12** and its negative control **13** as the desired product. Ullman type C-N coupling of **14** and **15** gave intermediate **16**, which was converted to **17** by iodination. Warhead **19** was made by Suzuki coupling of **17** with 5-pyrimidinylboronic acid **18**, followed by Boc deprotection. The linker attached pomalidomide analogs **22a** and **22b** were synthesized following similar procedures as for **11a**. Amide coupling of **22a** and **22b** with warhead **19** afforded the desired compound **23** and its negative control **24**.

12 and 23 bind BRAF and BRAF-V600E with high affinity. Using the DiscoverX KINOMEscan platform, the binding affinities of the two degraders to wild type BRAF or BRAF-V600E mutant were compared with their corresponding warheads. Our results demonstrated that the affinities of **23** were

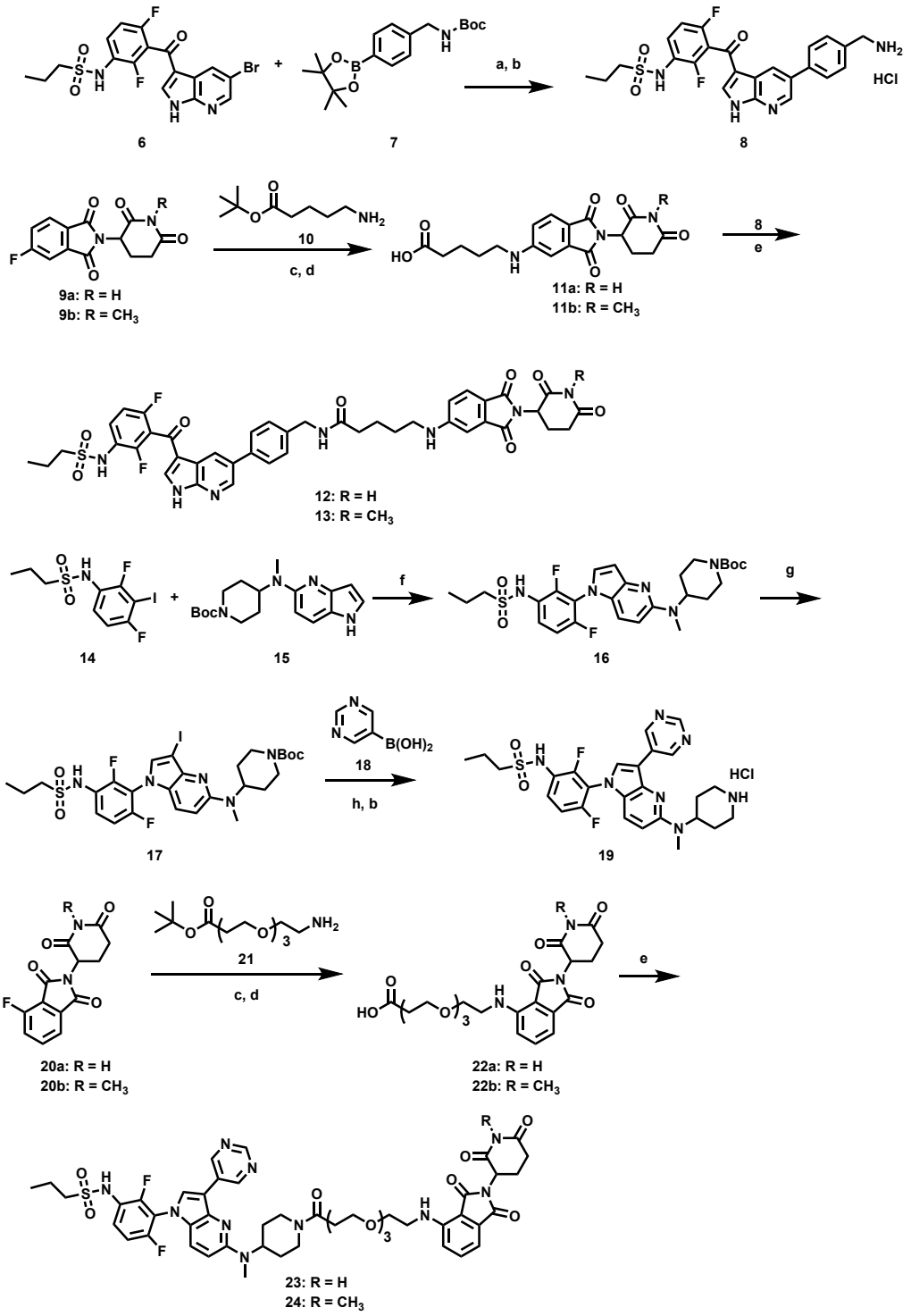

Scheme 1. Synthesis of **12** and **23** and their cereblon binding-deficient derivatives.

Reagents and conditions: (a) Pd(dppf)Cl_2, K_3PO_4, dioxane/H_2O, 80 °C, 6 h; (b) HCl/EtOAc, rt, overnight; (c) DIEA, NMP, microwave, 85 °C, 30 min; (d) TFA, rt, 2 h; (e) EDCI, HOAt, NMM, DMSO, rt, overnight; (f) CuI, (*R*,*R*)-*N*,*N'*-dimethyl-1,2-diaminocyclohexane, Cs_2CO_3, toluene, 120 °C, 48 h; (g) NIS, DMF/THF, rt, 1 h; (h) Pd(dppf)Cl_2, LiCl, Na_2CO_3, dioxane/H_2O, 100 °C, 1 h.

approximately 6-fold lower than those of BI882370 for both BRAF and BRAF-V600E mutant (Figure 2). In contrast, the affinities of **12** were 4- to 5-fold higher compared to vemurafenib (Figure 2), most likely due to the formation of an additional hydrogen bond between the amide carbonyl of **12** and the

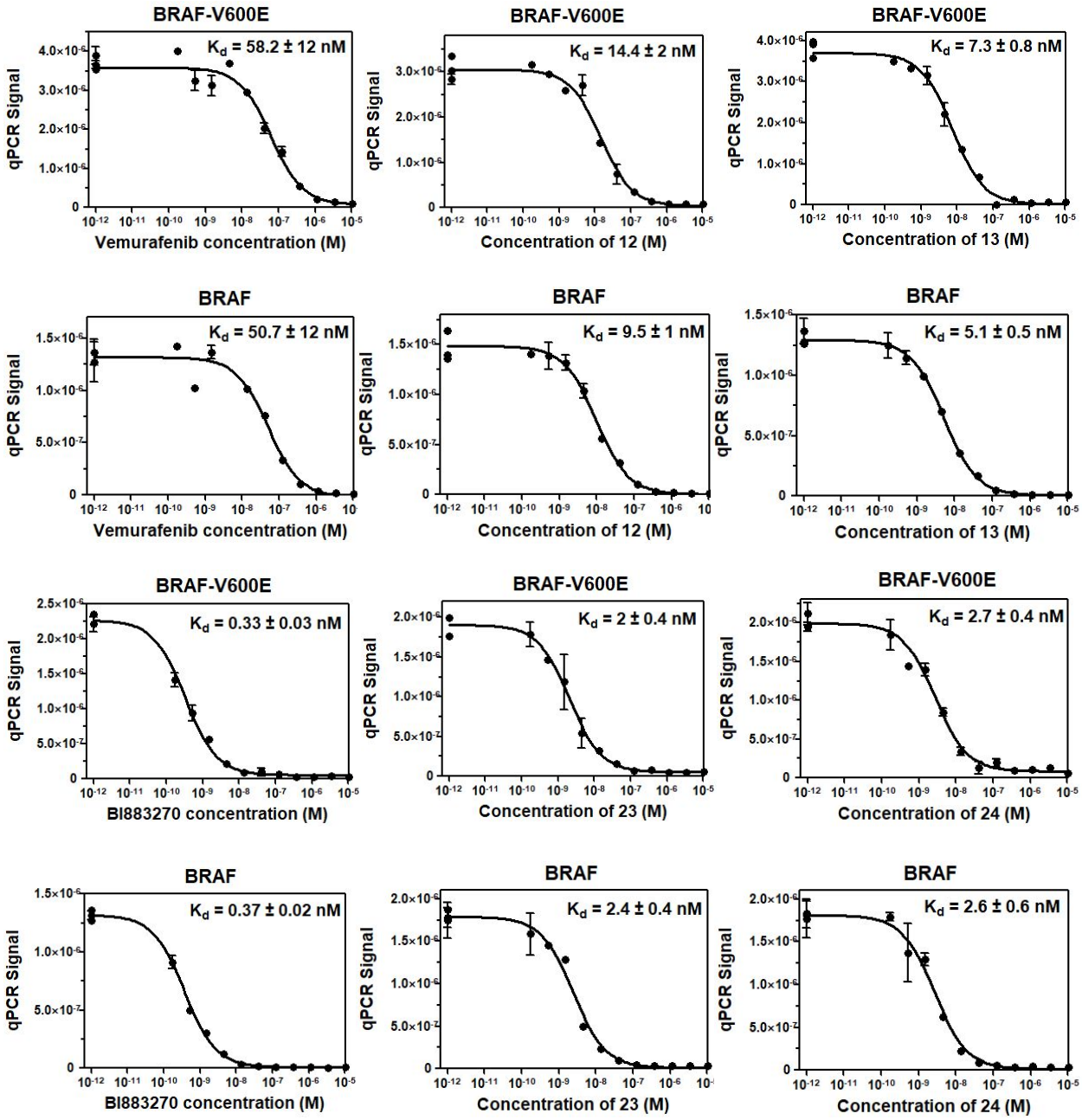

Figure 2. Binding affinities of vemurafenib, BI882370, degraders (**12**, **23**), and negative controls (**13**, **24**) to BRAF or BRAF-V600E. Binding affinities of individual compounds were determined using the KINOMEscan assay (DiscoveryX). The lowest concentration points represent data for the DMSO samples. Data are shown as mean ± SEM derived from duplicated independent experiments.

imidazole ring of His539 in BRAF as predicted by molecular modeling (Supporting Figure S1). Modifications to the thalidomide moiety by *N*-methylation (**13**, **24**) did not significantly affect affinities to either wild type BRAF or BRAF-V600E (Figure 2).

12 and 23 induce degradation of BRAF-V600E. The ability of **12** and **23** to degrade BRAF-V600E protein was first examined in A375 cells, a melanoma cell line homogeneously expressing BRAF-V600E. Cells were incubated with the degraders at various concentrations for 16 hours. For both degraders, reductions of BRAF-V600E protein levels were detected at 12 nM and intensified at higher concentrations, with the downstream ERK phosphorylation inhibited accordingly (Figure 3A and 3B). Moderate hook effects were observed at 1000 nM for both **12** and **23**, probably as excessive compounds undermined formation of the ternary complex of E3-degrader-BRAF-V600E. To determine the kinetics of BRAF-V600E degradation, we showed that significant depletion was not detected until 16 hours after degrader treatment (Figure 3C). However, reduction in the phosphorylation of ERK induced by **23** was detected as early as 2 h after incubation with cells, suggesting that degradation of BRAF-V600E was substantially delayed after binding of the degraders and the target protein.

In addition to BRAF-V600E, both vemurafenib and BI882370 are known to bind to the active form of wild type BRAF.[25] The KINOMEscan data also suggested that the degraders bound to wild type BRAF and BRAF-V600E with comparable affinities. Hence, we explored whether these degraders also degraded wild type BRAF using a lung cancer cell line, A549, in which BRAF is constantly activated by signals transduced from the oncogenic KRAS mutant. Our results demonstrated that neither **12** nor

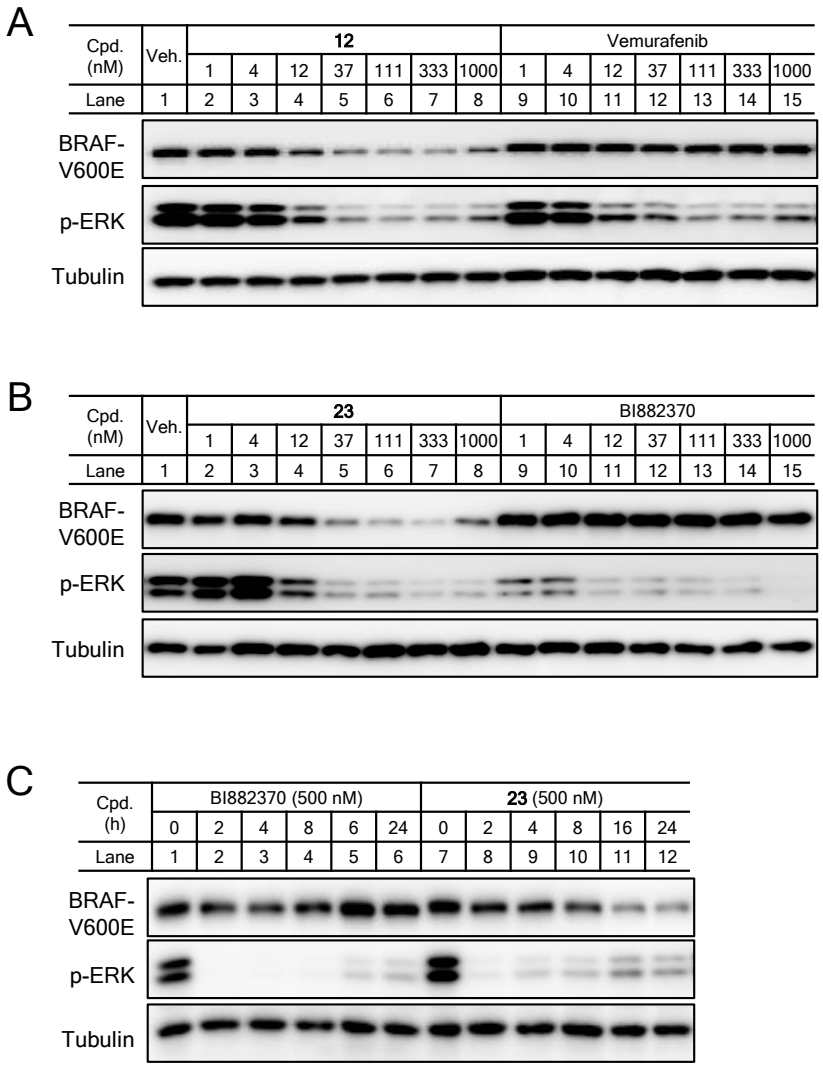

Figure 3. 12 and **23** induce degradation of BRAF-V600E. (A, B) A375 cells were treated with DMSO or serial dilutions of indicated compounds for 16 h. (C) A375 cells were treated with DMSO, 500 nM BI882370 or **23** for the indicated length of time.

23 resulted in significant degradation of wild type BRAF (Figure 4A and 4B), suggesting that binding

to the targeted protein is insufficient to induce degradation in the case of BRAF. To exclude influences

from variations in cellular context, we introduced expression of the kinase domain (residues: 448-723)

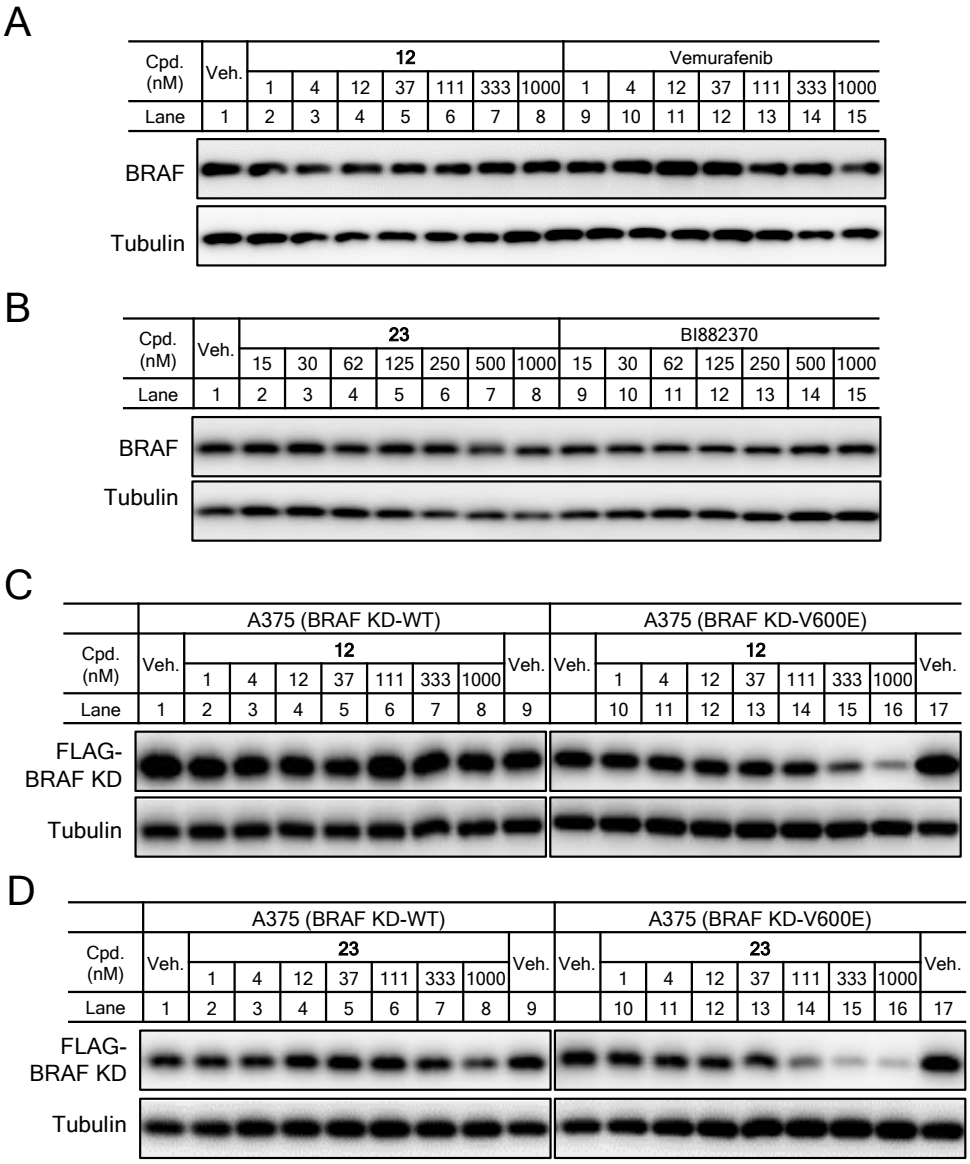

Figure 4. 12 and **23** do not degrade wild type BRAF. (A, B) A549 cells were treated with DMSO or indicated compounds following a 3-fold serial dilution for 16 h. (C, D) A375 cells stably expressing the kinase domain of BRAF or BRAF-V600E was treated with DMSO or indicated compounds for 16 hours following a 3-fold serial dilution. Levels of indicated proteins were shown using immunoblotting.

of BRAF-V600E or wild type BRAF into A375 cells. In line with the observations with full-length proteins, **12** and **23** selectively degraded the kinase domain of BRAF-V600E but not the wild type one (Figure 4C and 4D). These results collectively demonstrate that compounds **12** and **23** are potent and selective degraders for BRAF-V600E. However, there is a latency of degradation following binding

of the degraders and the target protein, which appeared to be longer than those for some of the reported degraders, such as BRD4[15], ALK[18], CDK4/6[19], and BRD7/9[20]. It is possible that our degraders require further optimization to facilitate the formation of productive ternary complexes comprising of E3 ligase, the degrader, and BRAF-V600E.

Degradation of BRAF-V600E is mediated by the ubiquitin-proteasome system. To confirm that the activities of our degraders were mediated via the cullin family E3 ligases and the UPS system, we employed multiple approaches to validate the mechanisms of BRAF-V600E targeted degradation. We generated derivatives of **12** and **23** that were deficient in binding to cereblon (Scheme 1). These negative control compounds, **13** and **24** respectively, were incapable of inducing degradation of BRAF-V600E in A375 cells (Figure 5A and 5B). However, their abilities of suppressing the downstream ERK phosphorylation were impaired but not blocked (Figure 5A and 5B), suggesting that the impact on downstream signaling for the degraders could result from both kinase inhibitory and protein degrading activities. We further demonstrated that degradation of BRAF-V600E induced by **12** and **23** could be rescued by pretreatment with proteasome inhibitors MG-132 or bortezomib (Figure 5C and 5D). Additionally, excessive amount of pomalidomide also counteracted the degrading activities of **12** and **23**, likely through competitive interaction with cereblon (Figure 5C and 5D). Similarly, pretreatment with MLN4929, an inhibitor of the NEDD8-activating enzyme (NAE) that suppresses the cullin family E3 ligases, also restored BRAF-V600E levels in the presence of **12** and **23** (Figure 5C and 5D). These results collectively validate a cullin-UPS-mediated mechanism for targeted degradation of BRAF-V600E.

Degradation of BRAF-V600E impairs melanoma cell growth. We next assessed the cellular

activities of BRAF-V600E degraders. In line with previous publications, BRAF kinase inhibitors

vemurafenib and BI882370 reduced viability of A375 cells (Figure 6A and 6B). The IC_{50} value of **23**

was approximately 10 times higher than its warhead, BI882370, while the IC_{50} of **24**, the cereblon

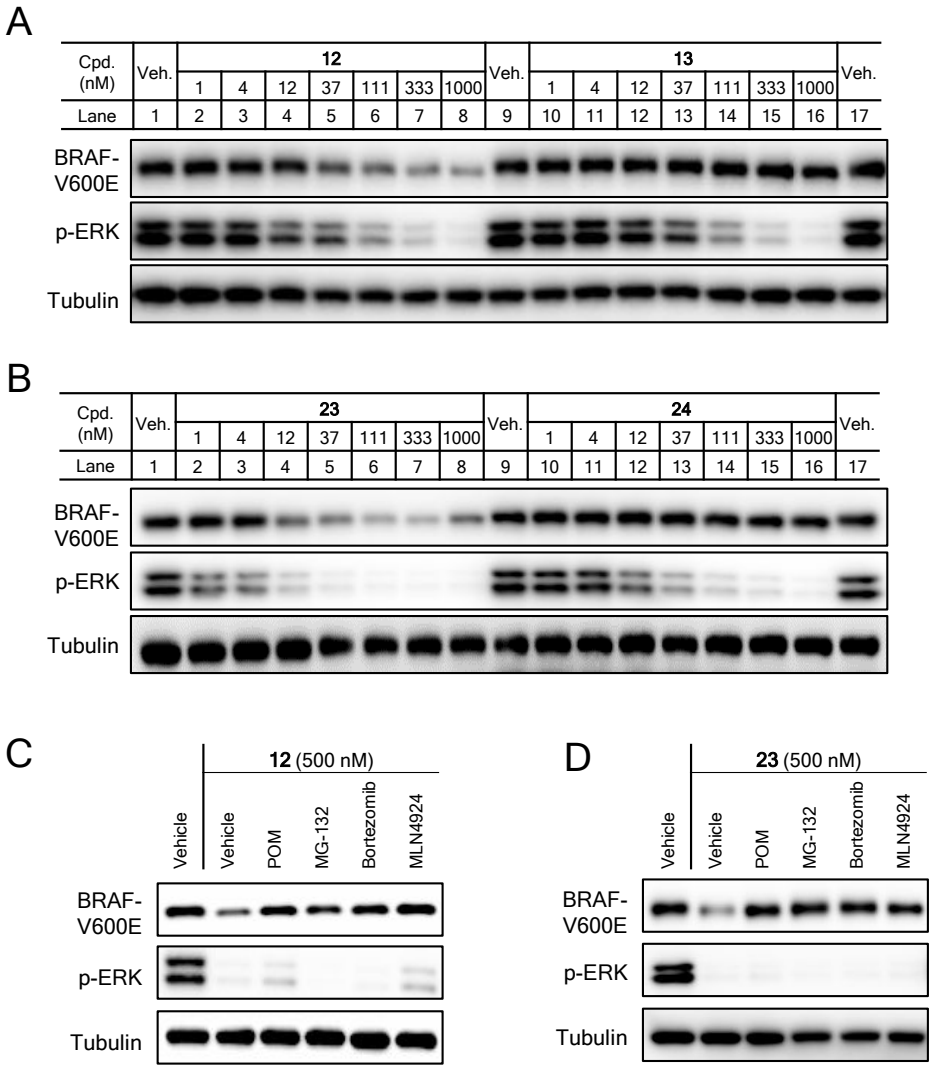

Figure 5. Degradation of BRAF-V600E is mediated by the ubiquitin-proteasome system (UPS). (A, B) A375 cells were treated with serial dilutions of compound **12**, **23**, or their respective negative controls **13** or **24** for 16 hours prior to immunoblotting. (C, D) A375 cells were pre-treated for 1 hour with DMSO, pomalidomide (POM, 10 μM), MG-132 (20 μM), bortezomib (200 nM) or MLN4924 (1 μM), and subsequently incubated with 500 nM **12** or **23** for 6 hours prior to immunoblotting.

binding-deficient derivative, was 4 times higher than **23**, suggesting that target degradation contributed

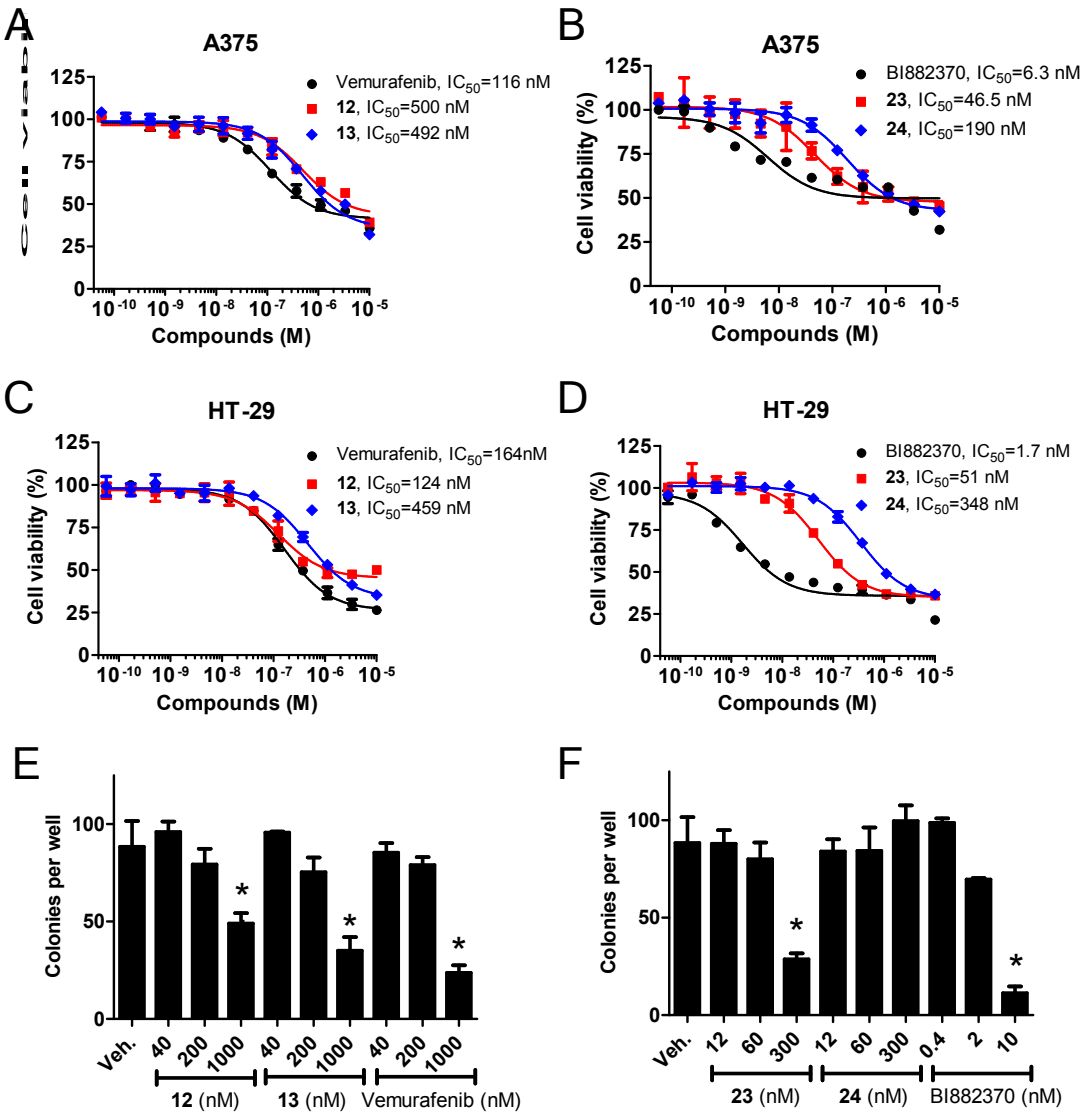

Figure 6. Degradation of BRAF-V600E impairs cell viability and colony formation. (A-D) Compound **12** and **23** reduced viability of A375 and HT-29 cells in a dose-dependent manner. (E, F) Compounds **12** and **23** inhibited colony formation of A375 cells. Data are shown as mean ± SD. *: $p < 0.05$ by Student's t-test compared with the corresponding control groups.

substantially to the cellular activity of **23** (Figure 6B). In contrast, the IC_{50} values of **12** and its non-degrading control **13** were similar (Figure 6A), suggesting that target degradation and kinase inhibition are implicated in the cellular activity of **12** to comparable extents. In the BRAF-V600E-dependent colon cancer cell line HT-29, these degraders and their negative controls induced similar patterns of growth inhibition, although the IC_{50} value of **12** appeared to be slightly lower in this line (Figure 6C

and 6D). These compounds as well as their warheads also impaired colony formation by A375 cells in a fashion resembling the observations in cell viability assays (Figure 6E and 6F). On the contrary, the degraders and their warheads did not induce significant loss of cell viability at physiologically concentrations in 3 non-neoplastic human cell lines (Supporting Figure S6). Taken together, our data suggest that selective degradation of BRAF-V600E by small molecule compounds impairs cell growth and viability in BRAF-V600E-driven melanoma and colon cancer cells.

Discussion and Conclusions

BRAF-V600E expression has been reported in a wide variety of human cancers. Mutations of BRAF are particularly common in melanoma, colon cancer, and thyroid cancer.[26] Additional aberrations that activate BRAF, such as alternative splicing and chromosomal translocation, have been increasingly recognized.[27] Multiple approved BRAF-V600E kinase inhibitors provide significant yet short-lived benefits to melanoma patients. In the current study, we report development of small molecule BRAF degraders. Degraders generated using VHL-1 as the E3 ligand were modestly active at best. In contrast, both thalidomide and pomalidomide yielded potent BRAF degraders with either vemurafenib or BI882370 as the warhead. Linker length had significant yet contrasting impact on the efficacy of degraders. Shorter linker length was associated with higher potency for degraders with vemurafenib as the warhead, while BI882370-based degraders required longer linker length in order to induce significant degradation. The development efforts were culminated in the discovery of two low-nanomolar degraders, **12** and **23**. These compounds selectively induced degradation of BRAF-V600E but not wild type BRAF, despite binding to both proteins with similar affinities. Mounting evidence

show that PROTAC compounds differentially degrade closely related target proteins,[28-31] suggesting that forming the ternary complex is necessary but insufficient to induce effective degradation of the target proteins. It has been well documented that BRAF kinase inhibitors bind to wild type BRAF and BRAF-V600E in distinct modes.[32] Hence, our results suggest that **12** and **23** may bind to BRAF-V600E in a conformation that favors the formation of cooperative ternary complex with the E3 complex, whereas they may form disruptive ternary complex with wild type BRAF. Following rapid binding to BRAF-V600E and blockade of the downstream MAPK kinase cascade, there were several hours of delay before significant degradation of BRAF-V600E could be detected. Therefore, the rate-limiting step of small molecule-induced proteolysis of BRAF-V600E is likely not the formation of the degrader-BRAF-V600E binary complex. Additional data, particularly crystal structures, will be required to fully address how **12** and **23** differentially target wild type BRAF and BRAF-V600E mutant.

In BRAF-V600E-dependent melanoma cells and colon cancer cells, **12** and **23** provoked *in vitro* antineoplastic activities comparable to clinical stage BRAF kinase inhibitors, but not in non-neoplastic human cells. Further studies are required to optimize the physiochemical properties of these novel degraders for preclinical and clinical development. Their activities should also be characterized in a wider range of BRAF-V600E-expressing cells. While the kinase activity has been well documented to be essential for the oncogenic potential of BRAF-V600E, kinase-independent activities of wild type BRAF and BRAF mutants have been described in various diseases.[33-36] Thus, the development of BRAF-V600E selective degraders provides a platform to systemically investigate the impact of depleting oncogenic BRAF mutants in human cancers.

Experimental Section

General Chemistry Methods. All chemicals and reagents were purchased from commercial suppliers and used without further purification. LCMS spectra for all compounds were acquired using a Shimadzu LC-MS 2020 system comprising a pump (LC-20AD) with degasser (DGU-20A3), an autosampler (SIL-20AHT), a column oven (CTO-20A) (set at 40 °C, unless otherwise indicated), a photo-diode array (PDA) (SPD-M20A) detector, an evaporative light-scattering (ELSD) (Alltech 3300ELSD) detector. Chromatography was performed on a Shimadzu SunFire C18 (5 μm 50 * 4.6mm) with water containing 0.1% formic acid as solvent A and acetonitrile containing 0.1% formic acid as solvent B at a flow rate of 2.0 mL/min. Flow from the column was split to a MS spectrometer. The MS detector was configured with an electrospray ionization source. Nitrogen was used as the nebulizer gas. Data acquisition was performed with a Labsolution data system. Proton Nuclear Magnetic Resonance (^{1}H-NMR) spectra were recorded on a Bruker Avance Ⅲ400 spectrometer. Chemical shifts are expressed in parts per million (ppm) and reported as δ value (chemical shift δ). Coupling constants are reported in units of Hertz (*J* value, Hz; integration and splitting patterns: where s = singlet, d = double, t = triplet, q = quartet, brs = broad singlet, m = multiple). Preparative HPLC was performed on Agilent Prep 1260 series with UV detector set to 254 nm or 220 nm. Samples were injected onto a Phenomenex Luna 75 x 30 mm, 5 μm, C18 column at room temperature. The flow rate was 40 mL/min. A linear gradient was used with 10% (or 50%) of MeOH (A) in H_2O (with 0.1 % TFA) (B) to 100% of MeOH (A). All compounds showed > 95% purity using the LCMS methods described above. Purities of final compounds were confirmed by UPLC-MS.

Synthesis of 12, 13, 23, and 24

***N*-(3-(5-(4-(Aminomethyl)phenyl)-1*H*-pyrrolo[2,3-*b*]pyridine-3-carbonyl)-2,4-difluorophenyl)propane-1-sulfonamide hydrochloride (8).** To a solution of *N*-(3-(5-bromo-1*H*-pyrrolo[2,3-*b*] pyridine-3-carbonyl)-2,4-difluorophenyl) propane-1-sulfonamide (2 g, 4.36 mmol) in 1,4-dixoane (100 mL) were added *tert*-butyl 4-(4,4,5,5-tetramethyl-1,3,2-dioxaborolan-2-yl)benzylcarbamate (1.45 g, 4.36 mmol), K_3PO_4 (2.32 g, 10.91 mmol) in water (30 mL), and [1,1'-bis(diphenylphosphino)ferrocene] dichloropalladium(II) (200 mg, 10% wt). After the reaction mixture was heated to 80 °C for 6 h, it was diluted with EtOAc (50 mL), washed with 5% lithium chloride aqueous solution (3 x 20 mL), and brine (20 mL). The organic layer was dried over Na_2SO_4, filtered, and concentrated in vacuo. The resulting residue was purified by silica gel column chromatography (petroleum ether: EtOAc = 1:4) to afford *tert*-butyl 4-(3-(2,6-difluoro-3-(propylsulfonamido) benzoyl)-1*H*-pyrrolo [2,3-*b*]pyridin-5-yl)benzylcarbamate (1.3 g, yield: 51%) as an off-white solid. MS (ESI) *m/z*: 585 $[M+H]^+$. ^{1}HNMR (400 MHz, DMSO-d_6) δ 12.98 (s, 1H), 9.76 (s, 1H), 8.70 (d, J = 2.4 Hz, 1H), 8.61 (s, 1H), 8.28 (s, 1H), 7.71 (d, J = 8.0 Hz, 2H), 7.62 – 7.56 (m, 1H), 7.45 (t, J = 6.0 Hz, 1H), 7.39 (d, J = 8.0 Hz, 2H), 7.31 – 7.26 (m, 1H), 4.20 (d, J = 6.0 Hz, 2H), 3.14 – 3.11 (m, 2H), 1.77 (dd, J = 8.0 Hz, 13.2, 2H), 1.42 (s, 9H), 0.97 (t, J = 7.2 Hz, 3H).

A mixture of *tert*-butyl 4-(3-(2,6-difluoro-3-(propylsulfonamido)benzoyl)-1*H*-pyrrolo[2,3-*b*]pyridin- 5-yl)benzylcarbamate (1.25 g, 2.14 mmol) and HC1 acid in EtOAc (3 M, 10 mL) was stirred at room temperature overnight. The reaction mixture was filtered to give the crude product, which was washed with EtOAc and dried in vacuum to afford the title compound (1.06 g, yield: 95%) as an off-white solid. MS (ESI) m/z: 485 $[M+H]^+$. ^{1}HNMR (400 MHz, DMSO-d_6) δ 13.10 (s, 1H), 9.80 (s, 1H),

8.74 (d, J = 2.4 Hz, 1H), 8.67 (s, 1H), 8.54 (br, 3H), 8.23 (s, 1H), 7.83 (d, J = 8.4 Hz, 2H), 7.66 (d, J = 8.0 Hz, 2H), 7.61 – 7.57 (m, 1H), 7.31 – 7.27 (m, 1H), 4.10 (q, J = 5.6 Hz, 2H), 3.16 – 3.20 (m, 2H), 1.78 – 1.72 (m, 2H), 0.97 (t, J = 7.2 Hz, 3H).

5-((2-(2,6-Dioxopiperidin-3-yl)-1,3-dioxoisoindolin-5-yl)amino)pentanoic acid (11a). A mixture of 2-(2,6-dioxopiperidin-3-yl)-5-fluoroisoindoline-1,3-dione (6.6 g, 24.0 mmol), *tert*-butyl 5-aminopentanoate (5.0 g, 26.4 mmol) and DIEA (9.3 g, 72 mmol) in NMP (60 mL) was stirred at 140 °C in a microwave reactor for 30 min. After cooling down to room temperature, the mixture was poured into EtOAc (200 mL), washed with water (2 x 200 mL) and brine (200 mL). The organic phase was dried over anhydrous Na_2SO_4, filtered and concentrated. The resulting crude product was purified by silica gel chromatography (petroleum ether : EtOAc = 1:1) to give *tert*-butyl 5-((2-(2,6-dioxopiperidin-3-yl)-1,3-dioxoisoindolin-5-yl)amino)pentanoate (1.5 g, yield: 13%) as a yellow solid. MS (ESI) m/z: 374.1 $[M+H]^+$. A solution of *tert*-butyl 5-((2-(2,6-dioxopiperidin-3-yl) -1,3-dioxoisoindolin-5-yl)amino)pentanoate (1.5 g, 3.5 mmol) in TFA (15 mL) was stirred at room temperature for 1 h. The reaction mixture was concentrated and the residue was purified by silica gel chromatography (DCM : MeOH = 20:1) to give the title compound (660 mg, yield: 51%) as a yellow solid. MS (ESI) *m/z*: 374.1 $[M+H]^+$. ^{1}H NMR (400 MHz, DMSO-d_6) δ 12.03 (br, 1H), 11.05 (s, 1H), 7.55 (d, J = 8.4 Hz, 1H), 7.10 (t, J = 5.2 Hz, 1H), 6.94 (s, 1H), 6.83 (dd, J = 1.6 Hz, 8.4 Hz, 1H), 5.02 (dd, J = 5.6 Hz, 12.8 Hz, 1H), 3.17 – 3.16 (m, 2H), 2.92 – 2.83 (m, 1H), 2.60 – 2.53 (m, 2H), 2.26 – 2.25 (m, 2H), 2.01 – 1.98 (m, 1H), 1.60 – 1.59 (m, 4H).

5-((2-(1-Methyl-2,6-dioxopiperidin-3-yl)-1,3-dioxoisoindolin-5-yl)amino)pentanoic acid (11b). The title compound (41% yield over 2 steps) was synthesized according to procedures for the preparation of **11a** from 5-fluoro-2-(1-methyl-2,6-dioxopiperidin-3-yl)isoindoline-1,3-dione and *tert*-

butyl 5-aminopentanoate followed by tert-butyl ester deprotection. MS (ESI) m/z: 388.5 $[M+H]^+$.

_N_-(4-(3-(2,6-Difluoro-3-(propylsulfonamido)benzoyl)-1_H_-pyrrolo[2,3-_b_]pyridin-5-yl)benzyl)-5-((2-(2,6-dioxopiperidin-3-yl)-1,3-dioxoisoindolin-5-yl)amino)pentanamide (12). A solution of _N_-(3-(5-(4-(aminomethyl)phenyl)-1_H_-pyrrolo[2,3-_b_]pyridine-3-carbonyl)-2,4-difluorophenyl)propane-1- sulfonamide hydrochloride (10 mg, 0.019 mmol), 5-((2-(2,6-dioxopiperidin-3-yl)-1,3-dioxoisoindolin- 5-yl)amino)pentanoic acid (8.6 mg, 0.023 mmol), EDCI (5.94 mg, 0.031 mmol), HOAt (4.18 mg, 0.031 mmol) and NMM (12.53 mg, 0.12 mmol) in DMSO (3 mL) was stirred at room temperature overnight. The reaction solution was diluted with EtOAc (100 mL), washed with water (100 mL). The aqueous layer was extracted with EtOAc (50 mL). The combined organic layer was washed with brine twice, dried over Na_2SO_4, filtered and concentrated. The resulting residue was purified by Prep-TLC (DCM: MeOH = 10:1) to give the title compound (10 mg, 63% yield) as a white solid. ^{1}H NMR (400 MHz, DMSO-d_6) δ 8.71 (s, 1H), 8.60 (d, J = 2.0 Hz, 1H), 7.98 (s, 1H), 7.63 – 7.71 (m, 3H), 7.51 (d, J = 8.4 Hz, 1H), 7.43 (d, J = 8.4 Hz, 2H), 7.16 (t, J = 8.4 Hz, 1H), 6.95 (d, J = 1.6 Hz, 1H), 6.81 – 6.84 (m, 1H), 4.98 – 5.03 (m, 1H), 4.44 (s, 2H), 3.23 (t, J = 7.2 Hz, 2H), 3.11 (t, J = 8.0 Hz, 2H), 2.60 – 2.87 (m, 3H), 2.34 (t, J = 7.2 Hz, 2H), 2.01 – 2.08 (m, 1H), 1.74 – 1.90 (m, 4H), 1.66 – 1.73 (m, 2H), 1.03 (t, J = 7.2 Hz, 3H). ^{13}C NMR (100 MHz, DMSO-d_6) δ 181.7, 174.4, 173.3, 170.4, 168.3, 167.9, 154.7, 148.5, 143.8, 138.3, 137.9, 137.3, 134.5, 132.3, 129.5, 128.1, 127.1, 124.8, 118.2, 116.6, 116.5, 115.4, 112.0, 111.7, 105.2, 53.8, 48.9, 42.4, 35.2, 35.1, 31.7, 30.8, 30.4, 29.4, 29.3, 29.2, 29.1, 28.9, 27.9, 26.7, 25.5, 23.0, 22.4, 16.9, 11.8. HRMS calcd for $C_{42}H_{40}F_2N_7O_8S$ $[M+H^+]$ 840.2622, found 840.2628.

_N_-(4-(3-(2,6-Difluoro-3-(propylsulfonamido)benzoyl)-1_H_-pyrrolo[2,3-_b_]pyridin-5-

yl)benzyl)-5-((2-(1-methyl-2,6-dioxopiperidin-3-yl)-1,3-dioxoisoindolin-5-yl)amino)pentanamide (13). The title compound (28% yield) was synthesized according to the procedures for the preparation of **12** from *N*-(3-(5-(4-(aminomethyl)phenyl)-1*H*-pyrrolo[2,3-*b*]pyridine-3-carbonyl)-2,4-difluorophenyl)propane-1-sulfonamide hydrochloride and 5-((2-(1-methyl-2,6-dioxopiperidin-3-yl)-1,3-dioxoisoindolin-5-yl)amino) pentanoic acid. ^{1}H NMR (400 MHz, DMSO-d_6) δ 8.71 (s, 1H), 8.60 (s, 1H), 7.97 (s, 1H), 7.63 – 7.73 (m, 3H), 7.52 (d, *J* = 8.4 Hz, 1H), 7.42 (d, *J* = 8.0 Hz, 2H), 7.16 (t, *J* = 8.4 Hz, 1H), 6.95 (d, *J* = 1.6 Hz, 1H), 6.83 (d, *J* = 9.2 Hz, 1H), 5.01 – 5.05 (m, 1H), 4.44 (s, 2H), 3.24 (t, *J* = 6.8 Hz, 2H), 3.09 – 3.13 (m, 5H), 2.80 – 2.86 (m, 2H), 2.59 – 2.68 (m, 1H), 2.34 (t, *J* = 7.2 Hz, 2H), 2.00 – 2.05 (m, 1H), 1.76 – 1.90 (m, 4H), 1.68 – 1.73 (m, 2H), 1.03 (t, *J* = 7.2 Hz, 3H). ^{13}C NMR (100 MHz, DMSO-d_6) δ 181.7, 174.4, 172.3, 170.1, 168.3, 167.9, 154.7, 148.3, 143.6, 138.4, 137.9, 137.3, 134.6, 129.5, 128.2, 128.1, 127.2, 124.8, 118.3, 116.6, 116.5, 115.4, 112.0, 111.8, 105.2, 105.1, 53.8, 49.5, 42.4, 35.2, 31.7, 31.1, 30.4, 29.4, 29.3, 29.2, 29.1, 28.9, 27.9, 26.7, 25.9, 23.0, 22.3, 21.7, 16.9, 13.0, 11.7. HRMS calcd for $C_{43}H_{42}F_2N_7O_8S$ [M+H$^+$] 854.2778, found 854.2778.

***tert*-Butyl 4-((1-(2,6-difluoro-3-(propylsulfonamido)phenyl)-1*H*-pyrrolo[3,2-*b*]pyridin-5-yl)(methyl) amino)piperidine-1-carboxylate (16).** A mixture of *tert*-butyl 4-(methyl-(1*H*-pyrrolo[3,2-*b*]pyridin-5-yl) amino)piperidine-1-carboxylate (7.0 g, 21.21 mmol), *N*-(2,4-difluoro-3-iodophenyl) propane-1-sulfonamide (11.5 g, 31.82 mmol), cuprous iodide (806 mg, 4.24 mmol), (*R*,*R*)-*N*,*N*'-dimethyl-1,2-diaminocyclohexane (1.34 mL, 8.48 mmol), and cesium carbonate (20.8 g, 63.64 mmol) in dry toluene (30 mL) was stirred at 120 °C for 16 hours. After addition of cuprous iodide (806 mg, 4.24 mmol), (*R*,*R*)-*N*,*N*'-dimethyl-1,2-diaminocyclohexane (1.34 mL, 8.48 mmol), and cesium carbonate (20.8 g, 63.64 mmol) the reaction mixture was stirred for further 24 h. Upon removal of

solvent in vacuo, the residue was diluted with DCM and washed with sodium bicarbonate solution. The organic layer was dried over anhydrous sodium sulfate and filtered. The solvent was removed in vacuo and the residue was purified by silica gel column chromatography (petroleum ether: EtOAc = 2:1) to afford the title compound (5.5 g, yield: 46%) as a yellow solid. MS (ESI) *m/z*: 564 $[M+H]^+$. ^{1}HNMR (400 MHz, $CDCl_3$) δ 7.64 – 7.58 (m, 1H), 7.26 – 7.25 (m, 2H), 7.16 – 7.11 (m, 1H), 6.70 (d, *J* = 3.2 Hz, 1H), 6.53 (d, *J* = 9.2 Hz, 1H), 4.82 – 4.74 (m, 1H), 4.35 – 4.17 (m, 2H), 3.14 – 3.10 (m, 2H), 2.96 – 2.83 (m, 5H), 1.96 – 1.86 (m, 2H), 1.75 – 1.66 (m, 4H), 1.49 (s, 9H), 1.07 (t, *J* = 7.6 Hz, 3H).

***tert*-Butyl 4-((1-(2,6-difluoro-3-(propylsulfonamido)phenyl)-3-iodo-1*H*-pyrrolo[3,2-*b*]pyridin-5-yl) (methyl)amino)piperidine-1-carboxylate (17).** To a solution of *tert*-butyl 4-((1-(2,6-difluoro-3-(propylsulfonamido)phenyl)-1*H*-pyrrolo[3,2-*b*]pyridin-5-yl)(methyl)amino)piperidine-1-carboxylate (5.5 g, 9.75 mmol) in DMF (50 mL) and THF (1 mL) was added *N*-iodosuccinimide (2.4 g, 10.73 mmol). After the mixture was stirred at room temperature for 1 h, the reaction was diluted with DCM (30 mL) and washed with aqueous saturated $NaHCO_3$. The organic layer was dried over anhydrous Na_2SO_4, filtered and concentrated under reduced pressure. The resulting residue was purified by silica gel column chromatography (petroleum ether: EtOAc = 2:1) to afford the title compound (5.1 g, yield: 76%) as a yellow solid. MS (ESI) *m/z*: 690 $[M+H]^+$. ^{1}HNMR (400 MHz, $CDCl_3$) δ 7.66 – 7.60 (m, 1H), 7.33 (s, 1H), 7.21 (d, *J* = 9.2 Hz, 1H), 7.14 (t, *J* = 8.8 Hz, 1H), 6.55 (d, *J* = 8.8 Hz, 1H), 6.49 (s, 1H), 4.85 – 4.78 (m, 1H), 4.37 – 4.25 (m, 2H), 3.15 – 3.11 (m, 2H), 2.99 – 2.86 (m, 5H), 1.96 – 1.86 (m, 2H), 1.80 – 1.65 (m, 4H), 1.49 (s, 9H), 1.07 (t, *J* = 7.6 Hz, 3H).

***N*-(2,4-Difluoro-3-(5-(methyl(piperidin-4-yl)amino)-3-(pyrimidin-5-yl)-1*H*-pyrrolo[3,2-*b*]pyridin-1-yl)phenyl)propane-1-sulfonamide hydrochloride (19).** To a solution of *tert*-butyl 4-

((1-(2,6-difluoro-3-(propylsulfonamido)phenyl)-3-iodo-1*H*-pyrrolo[3,2-*b*]pyridin-5-yl)(methyl)amino)piperidine-1-carboxylate (5.7 g, 8.26 mmol) in 1,4-dioxane and water (2:1 mixture, 60 mL), was added pyrimidin-5-yl-boronic acid (3.07g, 24.78 mmol), [1,1'-bis(diphenylphosphino)ferrocene]dichloropalladium(II) (604 mg, 0.83 mmol), lithium chloride (1.7 g, 41.3 mmol) and sodium carbonate (2.6 g, 24.78 mmol). After the resulting mixture was stirred at 100 °C for 1 h, it was diluted with DCM and washed with sodium bicarbonate solution. The organic layer was dried over anhydrous sodium sulfate, filtered and concentrated. The residue was purified by column chromatography (petroleum ether: EtOAc = 1:9) to afford *tert*-butyl 4-((1-(2,6-difluoro-3-(propylsulfonamido)phenyl)-3-(pyrimidin-5-yl)-1*H*-pyrrolo[3,2-*b*]pyridin-5-yl)(methyl)amino)piperidine-1-carboxylate (2.2 g, yield: 41%) as a yellow solid. MS (ESI) *m/z*: 642 $[M+1]^+$. ^{1}HNMR (400 MHz, DMSO-d_6) δ 9.93 (s, 1H), 9.66 (s, 2H), 9.03 (s, 1H), 8.42 (s, 1H), 7.64 – 7.58 (m, 1H), 7.49 – 7.44 (m, 2H), 6.81 (d, J = 9.6 Hz, 1H), 4.59 – 4.53 (m, 1H), 4.16 – 4.13 (m, 2H), 3.19 – 3.15 (m, 2H), 2.94 – 2.83 (m, 5H), 1.80 – 1.59 (m, 6H), 1.43 (s, 9H), 0.85 (t, J = 7.2 Hz, 3H).

To a solution of *tert*-butyl 4-((1-(2,6-difluoro-3-(propylsulfonamido)phenyl)-3-(pyrimidin-5-yl)-1*H*- pyrrolo[3,2-*b*]pyridin-5-yl)(methyl)amino)piperidine-1-carboxylate (2.2 g, 3.43 mmol) in DCM/MeOH (5:1, 30 mL) was added HCl (3 M in EtOAc, 20 mL) and the mixture was stirred at room temperature for 3 h. After evaporation, the residue was diluted with EtOAc. The precipitate was collected by filtration and dried to give *N*-(2,4-difluoro-3-(5-(methyl(piperidin-4-yl)amino)-3-(pyrimidin-5-yl)-1*H*-pyrrolo[3,2-*b*]pyridin-1-yl)phenyl) propane-1-sulfonamide hydrochloride (1.9 g, yield: 96%) as a yellow solid. MS (ESI) m/z: 542 $[M+1]^+$. ^{1}HNMR (400 MHz, DMSO-d_6) δ 10.00 (s, 1H), 9.74 (s, 2H), 9.27 – 9.18 (m, 3H), 8.53 (s, 1H), 7.68 – 7.62 (m, 1H), 7.58 (d, J = 9.2 Hz, 1H), 7.51 – 7.46 (m, 1H), 6.94 (d, J = 9.2 Hz, 1H), 4.72 – 4.66 (m, 1H), 3.42 – 3.39 (m, 2H), 3.32 – 3.08 (m,

4H), 3.00 (s, 3H), 2.17 – 2.08 (m, 2H), 1.92 – 1.87 (m, 2H), 1.83 – 1.74 (m, 2H), 1.00 (t, *J* = 7.6 Hz, 3H).

3-(2-(2-(2-((2-(2,6-Dioxopiperidin-3-yl)-1,3-dioxoisoindolin-4-yl)amino)ethoxy)ethoxy) ethoxy) propanoic acid (22a). The title compound (8% yield over 2 steps) was synthesized by coupling of 2-(2,6-dioxopiperidin-3-yl)-4-fluoroisoindoline-1,3-dione and *tert*-butyl 3-(2-(2-(2-aminoethoxy)ethoxy) ethoxy)propanoate followed by TFA mediated tert-butyl ester deprotection according to the procedures for the preparation of compound **11a**.MS (ESI) *m/z*: 478.1 $[M+H]^+$. ^1H NMR (400 MHz, DMSO-d_6) δ 7.59 (d, *J* = 11.2 Hz, 1H), 7.23 (t, *J* = 6.8 Hz, 1H), 7.04 (d, *J* = 1.6 Hz, 1H), 7.04 (dd, *J* = 2.4 Hz, 11.2 Hz, 1H), 5.06 (dd, *J* = 7.2 Hz, 16.8 Hz, 1H), 3.64 – 3.57 (m, 8H), 3.54 – 3.48 (m, 4H), 3.40 – 3.38 (m, 2H), 2.92 – 2.89 (m, 1H), 2.64 – 2.54 (m, 2H), 2.42 – 2.38 (m, 2H), 2.05 – 2.01 (m, 1H).

3-(2-(2-(2-((2-(1-Methyl-2,6-dioxopiperidin-3-yl)-1,3-dioxoisoindolin-4-yl)amino)ethoxy)ethoxy)ethoxy)propanoic acid (22b). The title compound (60% yield over 2 steps) was synthesized by coupling of 4-fluoro-2-(1-methyl-2,6-dioxopiperidin-3-yl)isoindoline-1,3-dione and tert-butyl 3-(2-(2-(2-aminoethoxy) ethoxy)ethoxy)propanoate followed by tert-butyl ester deprotection according to the procedures for the preparation of **11a**. MS (ESI) m/z: 492.2 $[M+H]^+$.

***N*-(3-(5-((1-(3-(2-(2-(2-((2-(2,6-Dioxopiperidin-3-yl)-1,3-dioxoisoindolin-4-yl)amino)ethoxy)ethoxy)ethoxy)propanoyl)piperidin-4-yl)(methyl)amino)-3-(pyrimidin-5-yl)-1*H*-pyrrolo[3,2-*b*]pyridin-1-yl)-2,4-difluorophenyl)propane-1-sulfonamide (23).** The title compound (72% yield) was synthesized according to the procedures for the preparation of **12** from *N*-(2,4-Difluoro-3-(5-(methyl(piperidin-4-yl)amino)- 3-(pyrimidin-5-yl)-1*H*-pyrrolo[3,2-*b*]pyridin-1-yl)phenyl)propane-1-sulfonamide hydrochloride and 3-(2-(2-(2-((2-(2,6-dioxopiperidin-3-yl)-1,3-

dioxoisoindolin-4-yl)amino)ethoxy)ethoxy) ethoxy) propanoic acid. ^{1}H NMR (400 MHz, MeOD) δ 9.55 (s, 2H), 9.08 (s, 1H), 8.19 (s, 1H), 7.68 – 7.74 (m, 1H), 7.58 – 7.60 (m, 1H), 7.45 (t, *J* = 8.4 Hz, 1H), 7.31 – 7.36 (m, 1H), 6.92 – 7.00 (m, 3H), 4.96 – 5.03 (m, 1H), 4.60 – 4.80 (m, 2H), 4.18 (d, *J* = 14.0 Hz, 1H), 3.72 – 3.82 (m, 2H), 3.59 – 3.67 (m, 12H), 3.40 – 3.42 (m, 2H), 3.16 – 3.20 (m, 2H), 3.05 (s, 3H), 2.57 – 2.86 (m, 6H), 2.03 – 2.07 (m, 1H), 1.82 – 1.94 (m, 5H), 1.70 – 1.78 (m, 1H), 1.06 (t, *J* = 7.2 Hz, 3H). ^{13}C NMR (100 MHz, DMSO-d_6) δ 173.3, 170.5, 169.4, 169.2, 167.8, 156.5, 154.5, 154.0, 153.7, 153.3, 150.8, 146.9, 141.2, 136.7, 132.5, 131.1, 128.8, 128.2, 128.1, 125.7, 123.4, 123.3, 122.4, 117.9, 115.7, 115.5, 113.1, 112.9, 111.1, 109.7, 109.6, 70.3, 70.1, 69.3, 67.3, 54.2, 49.0, 45.0, 42.2, 41.1, 33.2, 32.6, 31.4, 29.3, 28.6, 22.6, 17.3, 13.1. HRMS calcd for $C_{48}H_{55}F_2N_{10}O_{10}S$ [M+H$^+$] 1001.3786, found 1001.3812.

***N*-(2,4-Difluoro-3-(5-(methyl(1-(3-(2-(2-(2-((2-(1-methyl-2,6-dioxopiperidin-3-yl)-1,3-dioxoisoindolin-4-yl)amino)ethoxy)ethoxy)ethoxy)propanoyl)piperidin-4-yl)amino)-3-(pyrimidin-5-yl)-1*H*-pyrrolo[3,2-*b*]pyridin-1-yl)phenyl)propane-1-sulfonamide (24).** The title compound (50% yield) was synthesized according to the procedures for the preparation of **12** from *N*-(2,4-difluoro-3-(5-(methyl (piperidin-4-yl)amino)-3-(pyrimidin-5-yl)-1*H*-pyrrolo[3,2-*b*]pyridin-1-yl)phenyl)propane-1-sulfonamide hydrochloride and 3-(2-(2-(2-((2-(1-methyl-2,6-dioxopiperidin-3-yl)-1,3-dioxoisoindolin-4-yl)amino)ethoxy) ethoxy)ethoxy)propanoic acid. ^{1}H NMR (400 MHz, DMSO-d_6) δ 9.92 (s, 1H), 9.65 (s, 2H), 9.03 (s, 1H), 8.42 (s, 1H), 7.55 – 7.64 (m, 2H), 7.45 – 7.49 (m, 2H), 7.13 (d, *J* = 8.4 Hz, 1H), 7.03 (d, *J* = 6.8 Hz, 1H), 6.81 (d, *J* = 9.2 Hz, 1H), 6.60 (s, 1H), 5.10 – 5.14 (m, 1H), 4.59 (d, *J* = 10.8 Hz, 1H), 4.05 (d, *J* = 12.0 Hz, 1H), 3.40 – 3.66 (m, 17H), 3.10 – 3.20 (m, 3H), 3.01 (s, 3H), 2.93 (s, 3H), 2.54 – 2.77 (m, 4H), 2.01 – 2.05 (m, 1H), 1.73 – 1.80 (m, 5H), 1.52 – 1.62 (m, 1H), 1.00 (t, *J* = 7.2 Hz, 3H). ^{13}C NMR (100 MHz, DMSO-d_6) δ 172.3, 170.3, 169.4, 169.1,

167.7, 159.0, 158.6, 156.0, 155.8, 154.0, 153.7, 146.9, 141.7, 136.7, 132.6, 129.6, 128.8, 127.7, 127.6, 124.4, 123.3, 123.2, 121.7, 117.9, 117.1, 116.1, 114.2, 113.0, 112.8, 111.1, 109.9, 109.7, 104.8, 70.3, 70.2, 69.3, 67.4, 54.2, 49.6, 45.4, 42.2, 41.4, 33.3, 31.6, 30.7, 29.6, 28.9, 27.0, 21.8, 17.3, 13.1. HRMS calcd for $C_{49}H_{57}F_2N_{10}O_{10}S$ [M+H$^+$] 1015.3942, found 1015.3944.

Binding affinity assays. BRAF binding affinities were determined by DiscoverX (San Diego, USA) using the KINOMEscan platform. KINOMEscan™ is based on a competition binding assay that quantitatively measures the ability of a compound to compete with an immobilized, active-site directed ligand. The assay is performed by combining three components: DNA-tagged BRAF; immobilized ligand; and a test compound. The ability of the test compound to compete with the immobilized ligand is measured via quantitative PCR of the DNA tag. K_ds were determined using an 11-point 3-fold compound dilution series (top concentration = 10 μM in this case) with three DMSO control points in duplicates. Some outlier data points were subtracted.

Cell culture and transfection. A375, HT-29, A549, HaCaT, WI-38 and IMR-90 cells were purchased from the Cell Line Bank of Chinese Academy of Sciences. All cells were cultured at 37 °C with 5% CO_2 in Dulbecco's Modified Eagle Medium (DMEM) supplemented with 10% fetal bovine serum (Gibco, Thermo Fisher). Cells were authenticated using the short tandem repeat (STR) assays by BioWing Applied Biotechnology, Shanghai. Mycoplasma contamination was excluded following a PCR-based method. Cell transfection was performed using Lipofectamine 2000 (Invitrogen) following the manufacturer's instructions. Stable cell lines were established by lentivirus transduction, selected and maintained in medium containing 1 μg/mL puromycin (Beyotime Biotechnology).

Antibodies and reagents. Mouse anti-BRAF antibody (sc-5284) was purchased from Santa Cruz Biotechnology. Mouse anti-p-ERK1/2 antibody (4696S) was purchase from Cell Signaling Technology. HRP-conjugated anti-α-Tubulin antibody was produced in house. The CellTiter-Lumi Assay kit was purchased from Beyotime Biotechnology, Beijing. Vemurafenib was purchased from MedKoo Biosciences, Morrisville, NC, USA. BI882370 was prepared following published procedures (WO2012/104388).

Immunoblotting. Cultured cells were washed with cold PBS once and lysed in cold RIPA buffer supplemented with protease inhibitors and phosphatase inhibitors (Beyotime Biotechnology). The solutions were then incubated at 4 °C for 30 min with gentle agitation to fully lyse cells. Cell lysates were centrifuged at 13,000 rpm for 10 min at 4 °C and pellets were discarded. Total protein concentrations in the lysates were determined following BCA assays (Beyotime Biotechnology). Cell lysates were mixed with Laemmli loading buffer to 1 x and heated at 99 °C for 5 min. Proteins were resolved on SDS-PAGE and visualized using Western ECL Substrate kits on a ChemiDoc MP Imaging system (Bio-Rad). Protein bands were quantitated using the Image Lab software provided by Bio-Rad.

Cell viability assay. Cells were seeded at a density of 2000 cells per well in 96-well assay plates and treated with test compounds following a 12-point serial dilution. Three days later, cell viability was determined using the CellTiter-Lumi assay kit according to the manufacturer's instructions. The dose-response curves and IC_{50} values were calculated using the GraphPad Prism software following a nonlinear regression (least squares fit) method.

Colony formation assay. A375 cells were plated at 200 cells per well in 6-well plates and treated the next day as indicated in Figure legend. Seven days after incubated with DMSO or indicated compounds,

cells were fixed and visualized using 0.5% crystal violet. Colonies were counted using the Image J software.

Statistical analyses. Data presented were mean ± standard deviation unless otherwise indicated. Statistical significance was determined using the GraphPad Prism 5.0 software. P values of less than 0.05 were considered significant.

Supporting Information

Figure S1, S2, S3, S4, S5, S6, compound information, and molecular string.

Corresponding Author Information

*Corresponding author: mplewe@cullgen.com (M.P.) and jialiang.wang@cullgen.com (J.W.)

Author Contributions

The manuscript was written through contributions of all authors. All authors have given approval to the final version of the manuscript. All authors are employees of Cullgen. The design, study conduct, and financial support for the research were provided by Cullgen.

Abbreviations used

DIEA, diisopropylethylamine; DMEM, Dulbecco's Modified Eagle Medium; EDCI, *N*-(3-dimethylaminopropyl)-*N*′-ethylcarbodiimide; ERK, extracellular signal regulated kinase; HOAt, 1-hydroxy-7-azabenzotrizaole; MAPK, mitogen-activated protein kinase; NIS, *N*-iodosuccinimide; NMM, *N*-methylmorpholine; NMP, *N*-methylpyrrolidone; PROTAC; proteolysis-targeting chimera; rt: room temperature; RAF, rapidly accelerated fibrosarcoma; UPS, ubiquitin proteasome system

Notes

Y. L. is the president and CEO of Cullgen and GNI Group. GNI group has a significant financial equity interest in Cullgen.

References

(1) Durrant, D. E.; Morrison, D. K. Targeting the Raf kinases in human cancer: the Raf dimer dilemma. *Br. J. Cancer.* **2018,** *118*, 3-8.

(2) Davies, H.; Bignell, G. R.; Cox, C.; Stephens, P.; Edkins, S.; Clegg, S.; Teague, J.; Woffendin, H.; Garnett, M. J.; Bottomley, W.; Davis, N.; Dicks, E.; Ewing, R.; Floyd, Y.; Gray, K.; Hall, S.; Hawes, R.; Hughes, J.; Kosmidou, V.; Menzies, A.; Mould, C.; Parker, A.; Stevens, C.; Watt, S.; Hooper, S.; Wilson, R.; Jayatilake, H.; Gusterson, B. A.; Cooper, C.; Shipley, J.; Hargrave, D.; Pritchard-Jones, K.; Maitland, N.; Chenevix-Trench, G.; Riggins, G. J.; Bigner, D. D.; Palmieri, G.; Cossu, A.; Flanagan, A.; Nicholson, A.; Ho, J. W.; Leung, S. Y.; Yuen, S. T.; Weber, B. L.; Seigler, H. F.; Darrow, T. L.; Paterson, H.; Marais, R.; Marshall, C. J.; Wooster, R.; Stratton, M. R.; Futreal, P. A. Mutations of the BRAF gene in human cancer. *Nature* **2002,** *417*, 949-954.

(3) Lavoie, H.; Therrien, M. Regulation of RAF protein kinases in ERK signalling. *Nat. Rev. Mol. Cell Biol.* **2015,** *16*, 281-298.

(4) Bollag, G.; Hirth, P.; Tsai, J.; Zhang, J.; Ibrahim, P. N.; Cho, H.; Spevak, W.; Zhang, C.; Zhang, Y.; Habets, G.; Burton, E. A.; Wong, B.; Tsang, G.; West, B. L.; Powell, B.; Shellooe, R.; Marimuthu, A.; Nguyen, H.; Zhang, K. Y.; Artis, D. R.; Schlessinger, J.; Su, F.; Higgins, B.; Iyer, R.; D'Andrea, K.; Koehler, A.; Stumm, M.; Lin, P. S.; Lee, R. J.; Grippo, J.; Puzanov, I.; Kim, K. B.; Ribas, A.; McArthur, G. A.; Sosman, J. A.; Chapman, P. B.; Flaherty, K. T.; Xu, X.; Nathanson, K. L.; Nolop, K. Clinical efficacy of a RAF inhibitor needs broad target blockade in BRAF-mutant melanoma. *Nature* **2010,** *467*, 596-599.

(5) Hauschild, A.; Grob, J. J.; Demidov, L. V.; Jouary, T.; Gutzmer, R.; Millward, M.; Rutkowski, P.; Blank, C. U.; Miller, W. H., Jr.; Kaempgen, E.; Martin-Algarra, S.; Karaszewska, B.; Mauch, C.;

Chiarion-Sileni, V.; Martin, A. M.; Swann, S.; Haney, P.; Mirakhur, B.; Guckert, M. E.; Goodman, V.; Chapman, P. B. Dabrafenib in BRAF-mutated metastatic melanoma: a multicentre, open-label, phase 3 randomised controlled trial. *Lancet* **2012,** *380*, 358-365.

(6) Koelblinger, P.; Thuerigen, O.; Dummer, R. Development of encorafenib for BRAF-mutated advanced melanoma. *Curr. Opin. Oncol.* **2018,** *30*, 125-133.

(7) Poulikakos, P. I.; Zhang, C.; Bollag, G.; Shokat, K. M.; Rosen, N. RAF inhibitors transactivate RAF dimers and ERK signalling in cells with wild-type BRAF. *Nature* **2010,** 464, 427-30.

(8) Fedorenko, I. V.; Paraiso, K. H.; Smalley, K. S. Acquired and intrinsic BRAF inhibitor resistance in BRAF V600E mutant melanoma. *Biochem. Pharmacol.* **2011,** *82*, 201-209.

(9) Su, F.; Viros, A.; Milagre, C.; Trunzer, K.; Bollag, G.; Spleiss, O.; Reis-Filho, J. S.; Kong, X.; Koya, R. C.; Flaherty, K. T.; Chapman, P. B.; Kim, M. J.; Hayward, R.; Martin, M.; Yang, H.; Wang, Q.; Hilton, H.; Hang, J. S.; Noe, J.; Lambros, M.; Geyer, F.; Dhomen, N.; Niculescu-Duvaz, I.; Zambon, A.; Niculescu-Duvaz, D.; Preece, N.; Robert, L.; Otte, N. J.; Mok, S.; Kee, D.; Ma, Y.; Zhang, C.; Habets, G.; Burton, E. A.; Wong, B.; Nguyen, H.; Kockx, M.; Andries, L.; Lestini, B.; Nolop, K. B.; Lee, R. J.; Joe, A. K.; Troy, J. L.; Gonzalez, R.; Hutson, T. E.; Puzanov, I.; Chmielowski, B.; Springer, C. J.; McArthur, G. A.; Sosman, J. A.; Lo, R. S.; Ribas, A.; Marais, R. RAS mutations in cutaneous squamous-cell carcinomas in patients treated with BRAF inhibitors. *N. Engl. J. Med.* **2012,** *366*, 207-215.

(10) Chapman, P. B.; Hauschild, A.; Robert, C.; Haanen, J. B.; Ascierto, P.; Larkin, J.; Dummer, R.; Garbe, C.; Testori, A.; Maio, M.; Hogg, D.; Lorigan, P.; Lebbe, C.; Jouary, T.; Schadendorf, D.; Ribas, A.; O'Day, S. J.; Sosman, J. A.; Kirkwood, J. M.; Eggermont, A. M.; Dreno, B.; Nolop, K.; Li, J.; Nelson, B.; Hou, J.; Lee, R. J.; Flaherty, K. T.; McArthur, G. A.; Group, B.-S. Improved survival with

vemurafenib in melanoma with BRAF V600E mutation. *N. Engl. J. Med.* **2011,** 364, 2507-2516.

(11) Long, G. V.; Stroyakovskiy, D.; Gogas, H.; Levchenko, E.; de Braud, F.; Larkin, J.; Garbe, C.; Jouary, T.; Hauschild, A.; Grob, J. J.; Chiarion Sileni, V.; Lebbe, C.; Mandala, M.; Millward, M.; Arance, A.; Bondarenko, I.; Haanen, J. B.; Hansson, J.; Utikal, J.; Ferraresi, V.; Kovalenko, N.; Mohr, P.; Probachai, V.; Schadendorf, D.; Nathan, P.; Robert, C.; Ribas, A.; DeMarini, D. J.; Irani, J. G.; Casey, M.; Ouellet, D.; Martin, A. M.; Le, N.; Patel, K.; Flaherty, K. Combined BRAF and MEK inhibition versus BRAF inhibition alone in melanoma. *N. Engl. J. Med.* **2014,** *371*, 1877-1888.

(12) Lai, A. C.; Crews, C. M. Induced protein degradation: an emerging drug discovery paradigm. *Nat. Rev. Drug Discov.* **2017,** *16*, 101-114.

(13) Jiang, B.; Wang, E. S.; Donovan, K. A.; Liang, Y.; Fischer, E. S.; Zhang, T.; Gray, N. S. Development of dual and selective degraders of cyclin-dependent kinases 4 and 6. *Angew. Chem. Int. Ed. Engl.* **2019,** *58*, 6321-6326.

(14) Lai, A. C.; Toure, M.; Hellerschmied, D.; Salami, J.; Jaime-Figueroa, S.; Ko, E.; Hines, J.; Crews, C. M. Modular PROTAC design for the degradation of oncogenic BCR-ABL. *Angew. Chem. Int. Ed. Engl.* **2016,** *55*, 807-810.

(15) Lu, J.; Qian, Y.; Altieri, M.; Dong, H.; Wang, J.; Raina, K.; Hines, J.; Winkler, J. D.; Crew, A. P.; Coleman, K.; Crews, C. M. Hijacking the E3 ubiquitin ligase cereblon to efficiently target BRD4. *Chem. Biol.* **2015,** *22*, 755-763.

(16) Qin, C.; Hu, Y.; Zhou, B.; Fernandez-Salas, E.; Yang, C. Y.; Liu, L.; McEachern, D.; Przybranowski, S.; Wang, M.; Stuckey, J.; Meagher, J.; Bai, L.; Chen, Z.; Lin, M.; Yang, J.; Ziazadeh, D. N.; Xu, F.; Hu, J.; Xiang, W.; Huang, L.; Li, S.; Wen, B.; Sun, D.; Wang, S. Discovery of QCA570 as an exceptionally potent and efficacious proteolysis targeting chimera (PROTAC) degrader of the

bromodomain and extra-Terminal (BET) proteins capable of inducing complete and durable tumor regression. *J. Med. Chem.* **2018**, *61*, 6685-6704.

(17) Remillard, D.; Buckley, D. L.; Paulk, J.; Brien, G. L.; Sonnett, M.; Seo, H. S.; Dastjerdi, S.; Wuhr, M.; Dhe-Paganon, S.; Armstrong, S. A.; Bradner, J. E. Degradation of the BAF complex factor BRD9 by heterobifunctional ligands. *Angew. Chem. Int. Ed. Engl.* **2017**, *56*, 5738-5743.

(18) Zhang, C.; Han, X. R.; Yang, X.; Jiang, B.; Liu, J.; Xiong, Y.; Jin, J. Proteolysis targeting chimeras (PROTACs) of naplastic Lymphoma Kinase (ALK). *Eur. J. Med. Chem.* **2018,** *151*, 304-314.

(19) Zhao, B.; Burgess, K. PROTACs suppression of CDK4/6, crucial kinases for cell cycle regulation in cancer. *Chem. Commun. (Cambridge, U. K.)* **2019,** *55*, 2704-2707.

(20) Zoppi, V.; Hughes, S. J.; Maniaci, C.; Testa, A.; Gmaschitz, T.; Wieshofer, C.; Koegl, M.; Riching, K. M.; Daniels, D. L.; Spallarossa, A.; Ciulli, A. Iterative design and optimization of initially inactive proteolysis targeting chimeras (PROTACs) identify VZ185 as a potent, fast, and selective von Hippel-Lindau (VHL) based dual degrader probe of BRD9 and BRD7. *J. Med. Chem.* **2019,** *62*, 699-726.

(21) Agianian, B.; Gavathiotis, E. Current insights of BRAF inhibitors in cancer. *J. Med. Chem.* **2018,** *61*, 5775-5793.

(22) Bollag, G, H. P.; Tsai, J.; Zhang, J; Ibrahim, P. N.; Cho, H.; Spevak, W.; Zhang, C.; Zhang ,Y, Habets, G, Burton, E. A., Wong, B.;Tsang, G.;, West, B. L.;, Powell, B.;, Shellooe, R.;, Marimuthu, A.;, Nguyen, H.; Zhang, K. Y.; Artis, D. R. Schlessinger, J.; Su, F.; Higgins, B.; Iyer, R.; D'Andrea, K. ; Koehler, A.; Stumm, M.; Lin, P. S., Lee, R. J.; Grippo, J.; Puzanov, I., Kim, K. B.; Ribas, A.; McArthur, G. A,; Sosman, J. A.; Chapman, P. B.; Flaherty, K. T.; Xu, X.; Nathanson, K. L.; Nolop, K. Clinical efficacy of a RAF inhibitor needs broad target blockade in BRAF-mutant melanoma. *Nature.* **2010,** *467,* 596-599

(23) Waizenegger, I. C.; Baum, A.; Steurer, S.; Stadtmuller, H.; Bader, G.; Schaaf, O.; Garin-Chesa, P.; Schlattl, A.; Schweifer, N.; Haslinger, C.; Colbatzky, F.; Mousa, S.; Kalkuhl, A.; Kraut, N.; Adolf, G. R. A Novel RAF kinase inhibitor with DFG-out-binding mode: high efficacy in BRAF-mutant tumor xenograft models in the absence of normal tissue hyperproliferation. *Mol. Cancer. Ther.* **2016,** *15*, 354-365.

(24) Grasso, M.; Estrada, M. A.;. Ventocilla, C.; Samanta, M.; Maksimoska, J.; Villanueva, J.; Winkler, J. D.; Marmorstein, R. Chemically linked vemurafenib inhibitors promote an inactive $BRAF^{V600E}$ Conformation. *ACS Chem. Biol.* **2016,** *11*, 2876-2888.

(25) Tsai, J.; Lee, J. T.; Wang, W.; Zhang, J.; Cho, H.; Mamo, S.; Bremer, R.; Gillette, S.; Kong, J.; Haass, N. K.; Sproesser, K.; Li, L.; Smalley, K. S.; Fong, D.; Zhu, Y. L.; Marimuthu, A.; Nguyen, H.; Lam, B.; Liu, J.; Cheung, I.; Rice, J.; Suzuki, Y.; Luu, C.; Settachatgul, C.; Shellooe, R.; Cantwell, J.; Kim, S. H.; Schlessinger, J.; Zhang, K. Y.; West, B. L.; Powell, B.; Habets, G.; Zhang, C.; Ibrahim, P. N.; Hirth, P.; Artis, D. R.; Herlyn, M.; Bollag, G. Discovery of a selective inhibitor of oncogenic B-Raf kinase with potent antimelanoma activity. *Proc. Natl. Acad. Sci. U.S.A.* **2008,** *105*, 3041-3046.

(26) Karoulia, Z.; Gavathiotis, E.; Poulikakos, P. I. New perspectives for targeting RAF kinase in human cancer. *Nat. Rev. Cancer* **2017,** *17*, 676-691.

(27) Dankner, M.; Rose, A. A. N.; Rajkumar, S.; Siegel, P. M.; Watson, I. R. Classifying BRAF alterations in cancer: new rational therapeutic strategies for actionable mutations. *Oncogene* **2018,** *37*, 3183-3199.

(28) Bondeson, D. P.; Smith, B. E.; Burslem, G. M.; Buhimschi, A. D.; Hines, J.; Jaime-Figueroa, S.; Wang, J.; Hamman, B. D.; Ishchenko, A.; Crews, C. M. Lessons in PROTAC Design from Selective Degradation with a Promiscuous Warhead. *Cell Chem. Biol.* **2018,** *25*, 78-87.

(29) Huang, H. T.; Dobrovolsky, D.; Paulk, J.; Yang, G.; Weisberg, E. L.; Doctor, Z. M.; Buckley, D. L.; Cho, J. H.; Ko, E.; Jang, J.; Shi, K.; Choi, H. G.; Griffin, J. D.; Li, Y.; Treon, S. P.; Fischer, E. S.; Bradner, J. E.; Tan, L.; Gray, N. S. A chemoproteomic approach to query the degradable kinome using a multi-kinase degrader. *Cell Chem. Biol.* **2018,** *25*, 88-99.

(30) Smith, B. E.; Wang, S. L.; Jaime-Figueroa, S.; Harbin, A.; Wang, J.; Hamman, B. D.; Crews, C. M. Differential PROTAC substrate specificity dictated by orientation of recruited E3 ligase. *Nat. Commun.* **2019,** *10*, 131.

(31) Brand, M.; Jiang, B.; Bauer, S.; Donovan, K. A.; Liang, Y.; Wang, E. S.; Nowak, R. P.; Yuan, J. C.; Zhang, T.; Kwiatkowski, N.; Muller, A. C.; Fischer, E. S.; Gray, N. S.; Winter, G. E. Homolog-selective degradation as a strategy to probe the function of CDK6 in AML. *Cell Chem. Biol.* **2019,** *26*, 300-306.

(32) Garnett, M. J.; Rana, S.; Paterson, H.; Barford, D.; Marais, R. Wild-type and mutant B-RAF activate C-RAF through distinct mechanisms involving heterodimerization. *Mol. Cell* **2005,** *20*, 963-969.

(33) Haling, J. R.; Sudhamsu, J.; Yen, I.; Sideris, S.; Sandoval, W.; Phung, W.; Bravo, B. J.; Giannetti, A. M.; Peck, A.; Masselot, A.; Morales, T.; Smith, D.; Brandhuber, B. J.; Hymowitz, S. G.; Malek, S. Structure of the BRAF-MEK complex reveals a kinase activity independent role for BRAF in MAPK signaling. *Cancer Cell* **2014,** *26*, 402-413.

(34) Kung, J. E.; Jura, N. Structural Basis for the non-catalytic functions of protein kinases. *Structure* **2016,** *24*, 7-24.

(35) Shaw, A. S.; Kornev, A. P.; Hu, J.; Ahuja, L. G.; Taylor, S. S. Kinases and pseudokinases: lessons from RAF. *Mol. Cell. Biol.* **2014,** *34*, 1538-1546.

(36) Wan, P. T.; Garnett, M. J.; Roe, S. M.; Lee, S.; Niculescu-Duvaz, D.; Good, V. M.; Jones, C. M.; Marshall, C. J.; Springer, C. J.; Barford, D.; Marais, R. Mechanism of activation of the RAF-ERK signaling pathway by oncogenic mutations of B-RAF. *Cell* **2004,** *116*, 855-867.

TOC Graphic

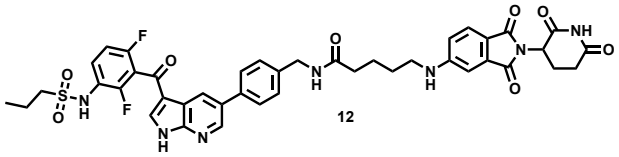

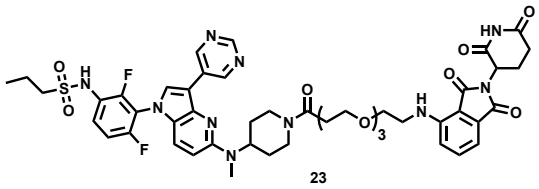

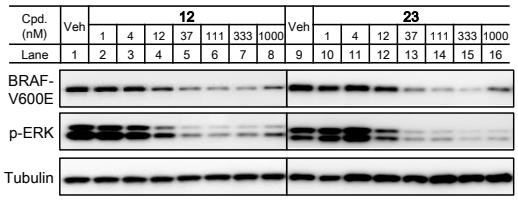

Legends

Scheme 1. Synthesis of **12** and **23** and their cereblon binding-deficient derivatives.

Reagents and conditions: (a) Pd(dppf)Cl_2, K_3PO4, dioxane/H2O, 80 °C, 6 h; (b) HCl/EtOAc, rt, overnight; (c) DIEA, NMP, microwave, 85 °C, 30 min; (d) TFA, rt, 2 h; (e) EDCI, HOAt, NMM, DMSO, rt, overnight; (f) CuI, (R,R)-N,N'-dimethyl-1,2-diaminocyclohexane, Cs_2CO_3, toluene, 120 °C, 48 h; (g) NIS, DMF/THF, rt, 1 h; (h) Pd(dppf)Cl_2, LiCl, Na_2CO_3, dioxane/H_2O, 100 °C, 1 h.

Figure 1. Chemical structures of **1** (vemurafenib), **2** (dabrafenib), **3** (encorafenib), **4** (BI882370) and **5** (Vem-bisamide-2).

Figure 2. Binding affinities of vemurafenib, BI882370, degraders (**12**, **23**), and negative controls (**13**, **24**) to BRAF or BRAF-V600E. Binding affinities of individual compounds were determined using the KINOMEscan assay (DiscoveryX). The lowest concentration points represent data for the DMSO samples. Data are shown as mean ± SEM derived from duplicated independent experiments.

Figure 3. **12** and **23** induce degradation of BRAF-V600E. (A, B) A375 cells were treated with DMSO or serial dilutions of indicated compounds for 16 h. (C) A375 cells were treated with DMSO, 500 nM BI882370 or **23** for the indicated length of time.

Figure 4. **12** and **23** do not degrade wild type BRAF. (A, B) A549 cells were treated with DMSO or indicated compounds following a 3-fold serial dilution for 16 h. (C, D) A375 cells stably expressing the kinase domain of BRAF or BRAF-V600E was treated with DMSO or indicated compounds for 16 hours following a 3-fold serial dilution. Levels of indicated proteins were shown using immunoblotting.

Figure 5. Degradation of BRAF-V600E is mediated by the ubiquitin-proteasome system (UPS). (A, B) A375 cells were treated with serial dilutions of compound **12**, **23**, or their respective negative controls **13** or **24** for 16 hours prior to immunoblotting. (C, D) A375 cells were pre-treated for 1 hour with DMSO, pomalidomide (POM, 10 μM), MG-132 (20 μM), bortezomib (200 nM) or MLN4924 (1 μM), and subsequently incubated with 500 nM **12** or **23** for 6 hours prior to immunoblotting.

Figure 6. Degradation of BRAF-V600E impairs cell viability and colony formation. (A-D) Compound **12** and **23** reduced viability of A375 and HT-29 cells in a dose-dependent manner. (E, F) Compounds

12 and **23** inhibited colony formation of A375 cells. Data are shown as mean ± SD. *: $p < 0.05$ by Student's t-test compared with the corresponding control groups.

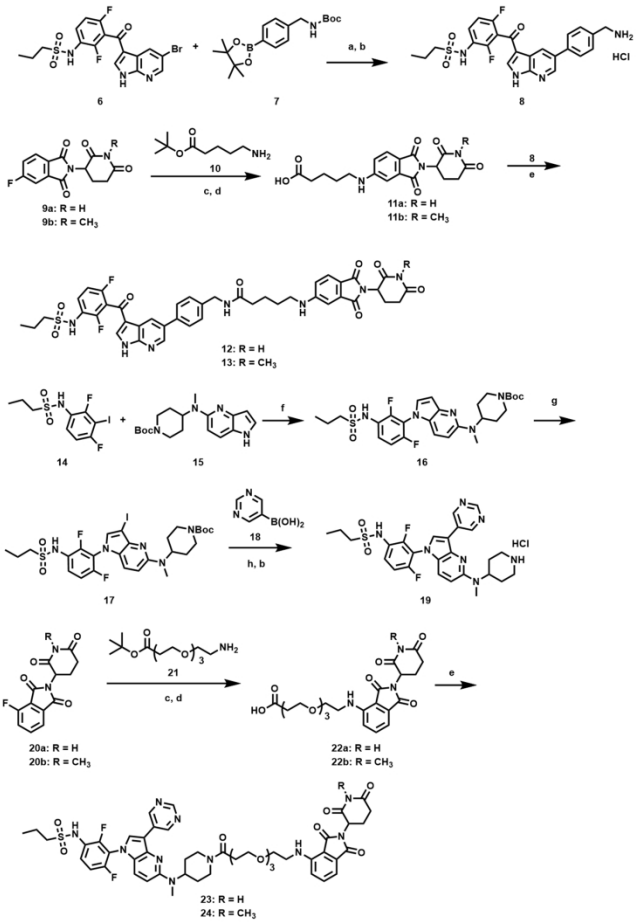

Scheme 1. Synthesis of **12** and **23** and their cereblon binding-deficient derivatives.

Scheme 1. Synthesis of 12 and 23 and their cereblon binding-deficient derivatives. Reagents and conditions: (a) Pd(dppf)Cl2, K3PO4, dioxane/H2O, 80 °C, 6 h; (b) HCl/EtOAc, rt, overnight; (c) DIEA, NMP, microwave, 85 °C, 30 min; (d) TFA, rt, 2 h; (e) EDCI, HOAt, NMM, DMSO, rt, overnight; (f) CuI, (R,R)-N,N'-dimethyl-1,2-diaminocyclohexane, Cs2CO3, toluene, 120 °C, 48 h; (g) NIS, DMF/THF, rt, 1 h; (h) Pd(dppf)Cl2, LiCl, Na2CO3, dioxane/H2O, 100 °C, 1 h.

190x254mm (300 x 300 DPI)

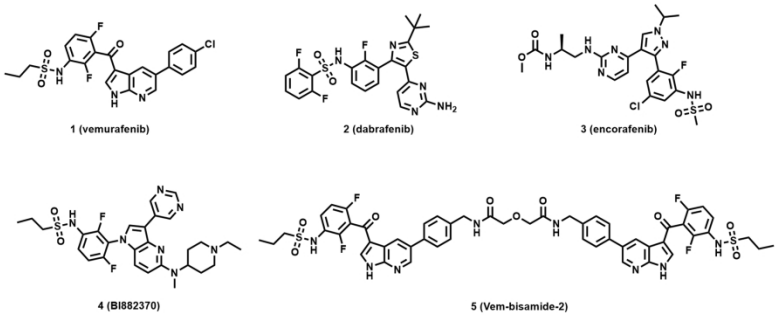

Figure 1. Chemical structures of **1** (vemurafenib), **2** (dabrafenib), **3** (encorafenib), **4** (BI882370) and **5** (Vem-bisamide-2).

Figure 1. Chemical structures of 1 (vemurafenib), 2 (dabrafenib), 3 (encorafenib), 4 (BI882370) and 5 (Vem-bisamide-2).

190x254mm (300 x 300 DPI)

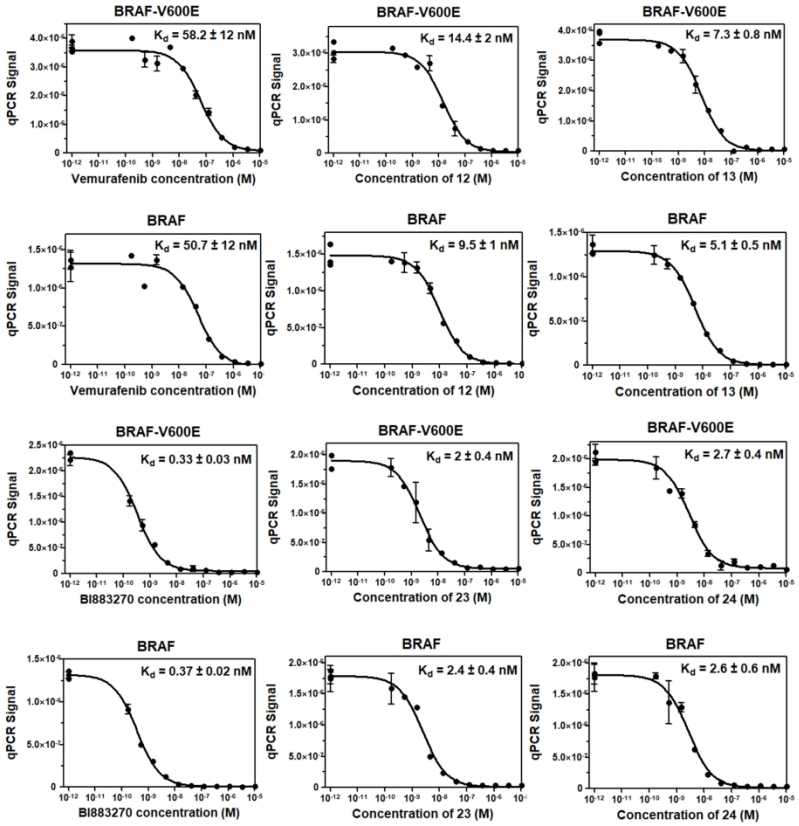

Figure 2. Binding affinities of vemurafenib, BI882370, degraders (**12**, **23**), and negative controls (**13**, **24**) to BRAF or BRAF-V600E.

Figure 2. Binding affinities of vemurafenib, BI882370, degraders (12, 23), and negative controls (13, 24) to BRAF or BRAF-V600E. Binding affinities of individual compounds were determined using the KINOMEscan assay (DiscoveryX). The lowest concentration points represent data for the DMSO samples. Data are shown as mean ± SEM derived from duplicated independent experiments.

190x254mm (300 x 300 DPI)

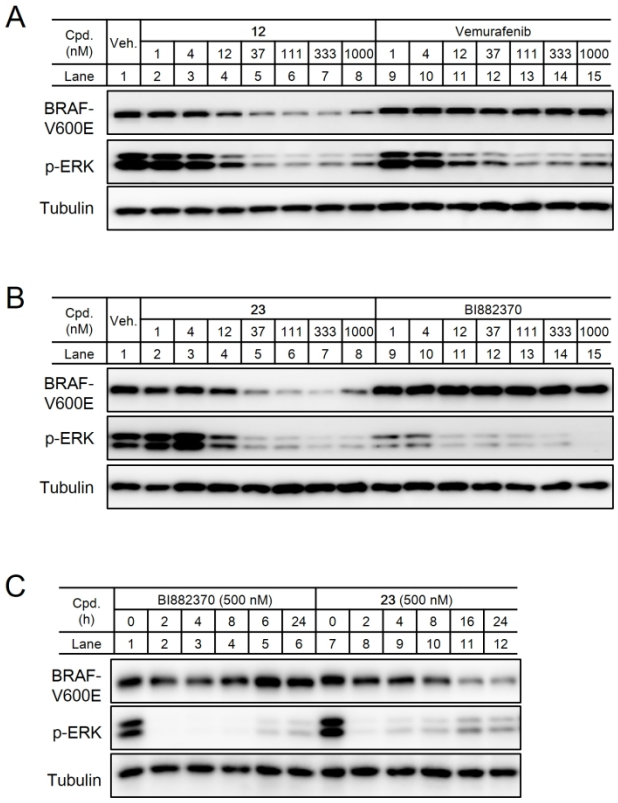

Figure 3. 12 and **23** induce degradation of BRAF-V600E.

Figure 3. 12 and 23 induce degradation of BRAF-V600E. (A, B) A375 cells were treated with DMSO or serial dilutions of indicated compounds for 16 h. (C) A375 cells were treated with DMSO, 500 nM BI882370 or 23 for the indicated length of time.

190x254mm (300 x 300 DPI)

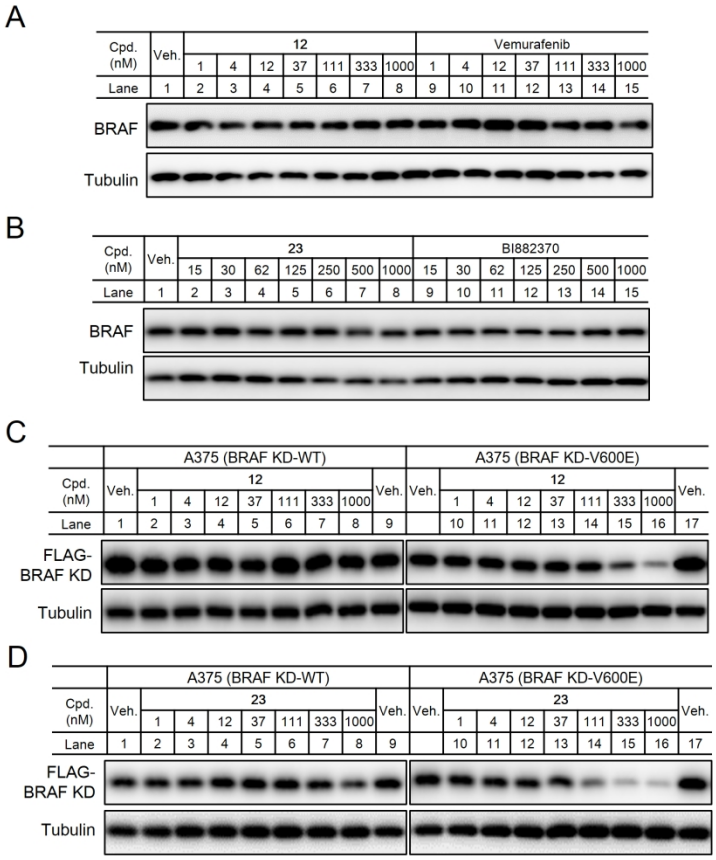

Figure 4. 12 and **23** do not degrade wild type BRAF.

Figure 4. 12 and 23 do not degrade wild type BRAF. (A, B) A549 cells were treated with DMSO or indicated compounds following a 3-fold serial dilution for 16 h. (C, D) A375 cells stably expressing the kinase domain of BRAF or BRAF-V600E was treated with DMSO or indicated compounds for 16 hours following a 3-fold serial dilution. Levels of indicated proteins were shown using immunoblotting.

190x254mm (300 x 300 DPI)

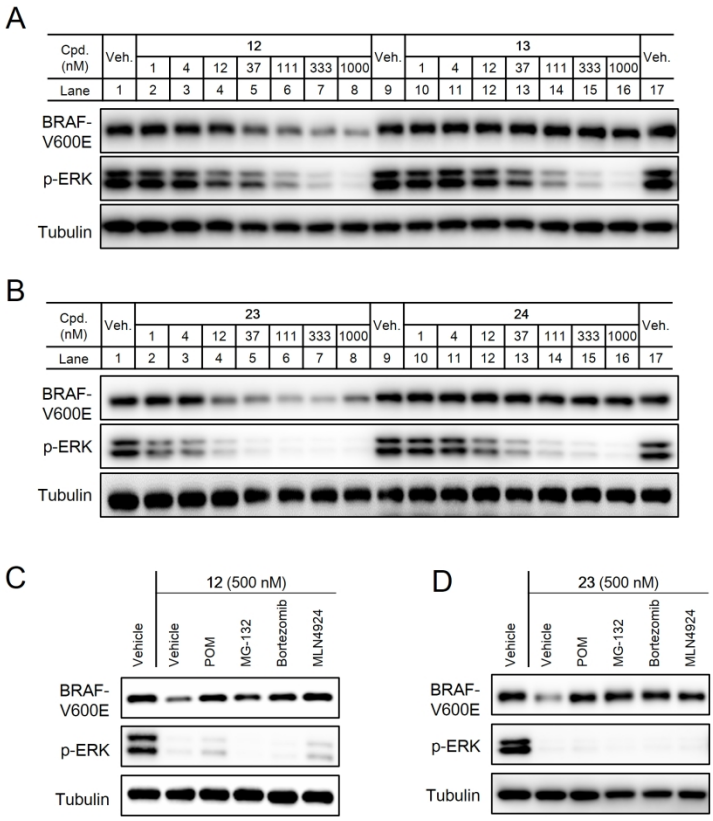

Figure 5. Degradation of BRAF-V600E is mediated by the ubiquitin-proteasome system (UPS).

Figure 5. Degradation of BRAF-V600E is mediated by the ubiquitin-proteasome system (UPS). (A, B) A375 cells were treated with serial dilutions of compound 12, 23, or their respective negative controls 13 or 24 for 16 hours prior to immunoblotting. (C, D) A375 cells were pre-treated for 1 hour with DMSO, pomalidomide (POM, 10 μM), MG-132 (20 μM), bortezomib (200 nM) or MLN4924 (1 μM), and subsequently incubated with 500 nM 12 or 23 for 6 hours prior to immunoblotting.

190x254mm (300 x 300 DPI)

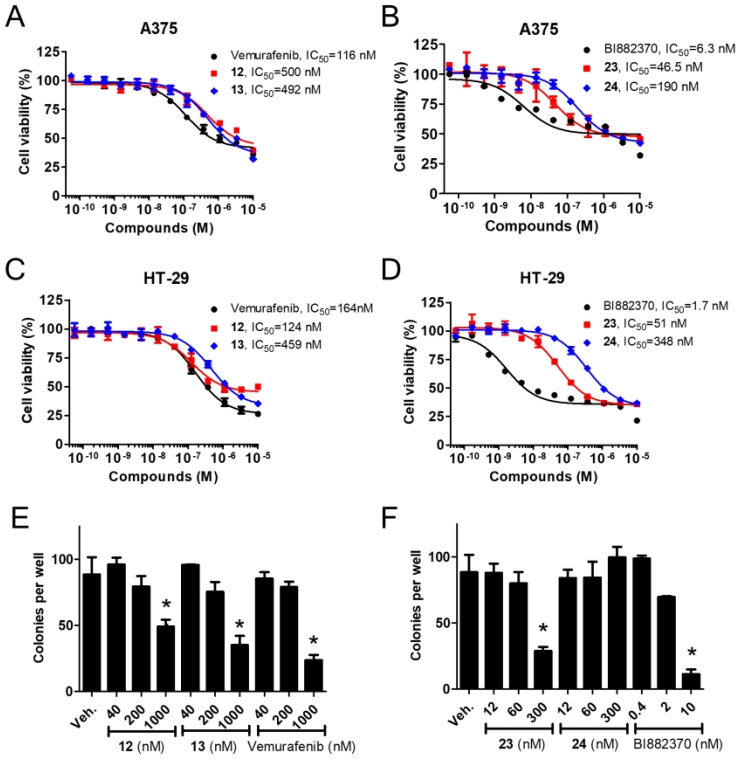

Figure 6. Degradation of BRAF-V600E impairs cell viability and colony formation. (A-D) Compound 12 and 23 reduced viability of A375 and HT-29 cells in a dose-dependent manner. (E, F) Compounds 12 and 23 inhibited colony formation of A375 cells. Data are shown as mean ± SD. *: $p < 0.05$ by Student's t-test compared with the corresponding control groups.

190x254mm (300 x 300 DPI)